Weierstraß-Institut
für Angewandte Analysis und Stochastik
Leibniz-Institut im Forschungsverbund Berlin e. V.

Preprint ISSN 2198-5855

Local equilibration error estimators for guaranteed error control in adaptive stochastic higher-order Galerkin FEM

Martin Eigel, Christian Merdon

submitted: August 20, 2014

Weierstrass Institute
Mohrenstr. 39
10117 Berlin
Germany
E-Mail: martin.eigel@wias-berlin.de
christian.merdon@wias-berlin.de

No. 1997
Berlin 2014

2010 *Mathematics Subject Classification.* 35R60,47B80,60H35,65C20,65N12,65N22,65J10.

Key words and phrases. Partial differential equations with random coefficients, equilibrated estimator, guaranteed bounds, uncertainty quantification, stochastic finite element methods, operator equations, adaptive methods.

Edited by
Weierstraß-Institut für Angewandte Analysis und Stochastik (WIAS)
Leibniz-Institut im Forschungsverbund Berlin e. V.
Mohrenstraße 39
10117 Berlin
Germany

Fax: +49 30 20372-303
E-Mail: preprint@wias-berlin.de
World Wide Web: http://www.wias-berlin.de/

ABSTRACT. Equilibration error estimators have been shown to commonly lead to very accurate guaranteed error bounds in the a posteriori error control of finite element methods for second order elliptic equations. Here, we extend previous results by designing equilibrated fluxes for higher-order finite element methods with nonconstant coefficients and illustrate the favourable performance of different variants of the error estimator within two deterministic benchmark settings.

After the introduction of the respective parametric problem with stochastic coefficients and the stochastic Galerkin FEM discretisation, a novel a posteriori error estimator for the stochastic error in the energy norm is devised. The error estimation is based on the stochastic residual and its decomposition into approximation residuals and a truncation error of the stochastic discretisation. Importantly, by using the derived deterministic equilibration techniques for the approximation residuals, the computable error bound is guaranteed for the considered class of problems. An adaptive algorithm allows the simultaneous refinement of the deterministic mesh and the stochastic discretisation in anisotropic Legendre polynomial chaos. Several stochastic benchmark problems illustrate the efficiency of the adaptive process.

INTRODUCTION

The a posteriori error analysis for conforming finite element methods for elliptic PDEs is well understood and analysed [38, 4, 26, 1, 8]. Moreover, even the design of guaranteed upper error bounds has been employed successfully for quite some time, see for instance [35, 18, 10, 12, 13]. Opposite to this, the a posteriori error control for numerical methods for PDEs with uncertain data has only just begun, see [19, 20, 6]. In addition to the approximation errors encountered in deterministic computations, stochastic problems usually lead to truncation errors due to the representation of stochastic fields in a finite number of random variables. Also, depending on the employed numerical method, the discretisation or sampling of the stochastic space introduces either additional approximation errors or uncertainties regarding the reliability of the obtained result. Ideally, with an adaptive numerical method, the different error contributions with regard to the current discrete approximation would be controlled such that the errors equilibrate in some sense. This necessitates the knowledge of computable reliable and efficient bounds for the different error components which has only been obtained in some cases so far.

Given sufficient regularity of the solution, the highest possible convergence rates can be achieved with projection or interpolation approaches, namely the stochastic Galerkin finite element method (SGFEM) [29, 28, 24] or quasi-spectral stochastic collocation (SC) [2, 3]. These methods however inevitably lead to high-dimensional algebraic systems. This severely limits their applicability to problems of practical interest. A lot of research is thus devoted to the reduction of the complexity of the discretisation. Theoretical results regarding the decay of coefficients of the stochastic data and the regularity of the stochastic solution have led to a priori adapted stochastic discretisations, see [23, 37, 3, 16, 37, 15, 17]. In particular, optimal convergence rates can be specified depending on the problem data. For a recent overview we refer to [36]. Moreover, heuristic adaptive procedures were mainly described for SC. For instance, a possibly beneficial refinement strategy can be deduced by the fitting of observed numerical convergence, see [32, 33]. Another approach which involves the solution of small auxiliary problems is described in [7]. Other promising approaches include the determination of an adequate set of base functions by the proper orthogonal decomposition or the reduced basis method [34, 14] and the representation of the discretisation in low-rank tensor formats [22, 30].

In this paper we pursue a different approach which is reminiscent of the systematic iterative construction of problem-adapted discretisation spaces in the deterministic finite element method. In contrast to the previously mentioned approaches, we exploit the orthogonality of the error of the approximate solution on the discrete space as a key benefit of the SGFEM. This unique property of the projection method is the pivotal feature which enables the development of reliable and even guaranteed a posteriori error estimates, as shown in this paper. In our opinion, this specific advantage over other methods clearly outweighs the somewhat higher computational costs and implementation effort whenever the SGFEM is feasible for the problem at hand.

We first consider the Poisson model problem that seeks $u \in V := H^1_0(D)$ with

$$-\nabla \cdot (a_0 \nabla u) = f \text{ in } D, \qquad u = 0 \text{ on } \partial D$$

on some Lipschitz domain $D \subset \mathbb{R}^d$ ($d = 2, 3$) with scalar diffusion coefficient $a_0 \in L^\infty(D)$. Note that our derivations hold equally for other equations, in particular second order linear elliptic equations, and more general boundary conditions.

The corresponding stochastic problem assumes the diffusion coefficient a to have the mean value a_0 and to depend on an infinite set of independent random variables. We reformulate the stochastic PDE as a parametric PDE on the parameter domain Γ. The probability product measure on Γ according to the random variables is denoted by π. For the discrete SGFEM approximation u_N of the exact solution $u \in \mathcal{V} := L^2_\pi(\Gamma; V) \simeq L^2_\pi(\Gamma) \otimes V$, an explicit residual-based a posteriori error estimator for the mean energy error

$$\|u - u_N\|^2_{L^2_\pi(\Gamma;V)} := \int_\Gamma \|u - u_N\|_{a_0} d\pi := \int_\Gamma \int_D a_0 |\nabla(u - u_N)|^2 \, dx d\pi$$

and the energy error

$$\|u - u_N\|^2_{\mathcal{A}} := \int_\Gamma \int_D a |\nabla(u - u_N)|^2 \, dx d\pi$$

was recently analysed in [19, 20]. The a posteriori error indicators derived there lead to a provably convergent adaptive algorithm for a certain class of stochastic problems. It is noteworthy that the proposed algorithm ensures a balanced refinement of the spatial as well as the stochastic discretisation.

Based on these results, this paper aims for guaranteed upper error bounds of both energy error norms for a higher-order SGFEM discretisation on the basis of equilibration error estimators in the spirit of [18, 10, 13]. For this, we derive the construction of global and local equilibrated fluxes for the deterministic equation. This result then is employed with the stochastic residual to obtain exact bounds for the discretisation error of the stochastic problem. A combination with some tail error indicator as a measure for the truncation of the expansion of the diffusion coefficient eventually leads to a guaranteed bound of the overall mean energy error.

The SGFEM discretisation assumes some expansion of the stochastic data which in our case is the random field $a(y, x) := a_0(x) + \sum_{m=1}^\infty a_m(x) y_m$ for $(y, x) \in \Gamma \times D$, an orthonormal basis of the parameter domain Γ with respect to the norm $\|\cdot\|_{L^2_\pi(\Gamma)}$, and a discrete basis of the physical domain D. For simplicity, we assume an affine dependence of a on the parameters $y := (y_m)_{m=1}^\infty \in \Gamma$ where the y_m are independent and uniformly distributed random variables with probability measures π_m. This leads to the product measure $\pi := \otimes_{m=1}^\infty \pi_m$ and a basis of $L^2_\pi(\Gamma)$ consisting of tensorised Legendre polynomials $(P_\mu)_{\mu \in \mathcal{F}}$ with the set $\mathcal{F}$ of compactly supported multi-indices. Hence, a representation of the solution $u \in \mathcal{V}$ is given

by $u(x,y) = \sum_{\mu\in\mathcal{F}} u_\mu(x)P_\mu(y)$ for $(x,y) \in D \times \Gamma$ with coefficients $u_\mu \in V$. The tensor product Hilbert space $\mathcal{V}$ allows for a separate discretisation of the deterministic space $V_h \subset V$ with finite element ansatz functions based on a partition of D and a finite dimensional subspace of the stochastic space $L^2_\pi(\Gamma)$ by the selection of a finite set of active modes $\Lambda \subset \mathcal{F}$ with $|\Lambda| < \infty$. With the associated polynomial basis P_μ, the discrete problem can be formulated as coupled subproblems such that the discrete solution $w_N \in \mathcal{V}_N := \operatorname{span}\{P_\mu\} \otimes V_h$ enjoys Galerkin orthogonality separately for each active stochastic mode $\nu \in \Lambda$ in the sense that

$$r_\nu(w_N)(v_h) := \int_D f_\nu v_h \, dx - \int_D \sigma_{h,\nu} \cdot \nabla v_h \, dx = 0 \quad \text{for all } v_h \in V_h \tag{0.1}$$

with some ν-dependent (deterministic) right-hand side f_ν and discrete stochastic stress $\sigma_{h,\nu}$ with respect to u_N. A detailed derivation of the weak formulation can be found in Section 4.

The prior works [19, 20] showed that the total mean energy error can be split into two residual parts, namely

$$\|u - u_N\|^2_{L^2_\pi(\Gamma;V)} = \|\mathcal{R}_\Lambda(w_N)\|^2_{L^2_\pi(\Gamma;V^*)} + \|\mathcal{R}_{\partial\Lambda}(w_N)\|^2_{L^2_\pi(\Gamma;V^*)} \tag{0.2}$$

with the stochastic residual $\mathcal{R}(w_N) := \mathcal{R}_\Lambda + \mathcal{R}_{\partial\Lambda}$. Here, $\partial\Lambda$ denotes the boundary of the active set Λ. The second term on the right-hand side of (0.2) is a tail (or truncation) error indicator for the set of inactive modes, while the first approximation term further decomposes as

$$\|\mathcal{R}(w_N)\|^2_{L^2_\pi(\Gamma;V^*)} = \sum_{\nu\in\mathcal{F}} \|r_\nu(w_N)\|^2_{V^*} \tag{0.3}$$

into to the dual norms $\|r_\nu(w_N)\|_{V^*} := \sup_{v\in V\setminus\{0\}} r_\nu(w_n)/\|v\|_{a_0}$ of the single mode residuals r_ν from (0.1). Their Galerkin orthogonality allows for the application of local equilibration error estimators to estimate the dual norm of the residual r_ν.

This paper extends the local equilibration error estimator designs of [18, 10, 13] to higher-order finite element methods and nonconstant diffusion coefficients which is especially required for the application in stochastic problems. Their efficiency in the discrete and stochastic cases is verified in several numerical benchmark examples with uniform and adaptive mesh refinement.

In the stochastic applications, the adaptive algorithm not only controls the mesh refinement of the spatial discretisation but also the stochastic tail error, i.e. the set of active stochastic modes and thus the discretisation and approximation quality of the stochastic space.

The outline of this paper is as follows. Section 1 starts with the formulation of the deterministic problem with possibly nonconstant diffusion parameter a_0 (e.g. the mean value of the diffusion coefficient a in the later stochastic setting). Section 2 explains our equilibration error estimators which include some novelties with respect to local equilibration for higher-order finite element methods and nonconstant a_0. The presentation is complemented by an extensive comparison of the derived estimators in two settings, the L-shaped domain with constant coefficient and the unit square with inhomogeneous coefficient. Section 3 introduces the stochastic setting, in particular the polynomial chaos expansion of the stochastic space. Section 4 provides details about the stochastic Galerkin finite element discretisation based on the variational formulation of the stochastic problem as parametric PDE. In Section 5, we express the energy mean error in terms of dual norms of stochastic residuals and their separation into deterministic residuals of stochastic modes. With these, in Section 6 guaranteed explicit upper error bounds by application of the deterministic equilibration error estimators of Section 2 to bound the local mode-dependent deterministic residuals are designed. An adaptive algorithm which is steered by the derived

error bounds is described in Section 7. Section 8 concludes the paper with a set of numerical stochastic benchmark examples which illustrate the performance of the new exact a posteriori error estimator.

1. DETERMINISTIC SETTING

This section introduces the Poisson equation as a model problem for the derivation of guaranteed error upper bounds. Additionally, we briefly recall the treatment of inhomogeneous Dirichlet data.

1.1. **Poisson model problem.** The deterministic Poisson model problem with deterministic coefficients on some Lipschitz domain $D \subset \mathbb{R}^d$, $d \in \{2, 3\}$, seeks $u \in V := H^1_0(D) := \{v \in H^1(D) : v|_{\partial D} = 0\}$ with

$$-\nabla \cdot (a_0 \nabla u) = f \text{ in } D, \qquad u = 0 \text{ on } \partial D \tag{1.1}$$

for some right-hand side $f \in L^2(D)$ and diffusion coefficient $a_0 \in L^\infty(D)$ that is uniformly bounded from below by

$$0 < a_{\min} < \operatorname*{ess\,inf}_{x \in D} a_0(x). \tag{1.2}$$

The weak formulation employs the a_0-weighted inner product

$$(u, v)_V := \int_D a_0(x) \nabla u(x) \cdot \nabla v(x)\, dx \quad \text{for } u, v \in V$$

which induces the energy norm $\|v\|^2_{a_0} := (v, v)_V$.

1.2. **Discretisation and residual.** For the discretisation consider a regular triangulation $\mathcal{T}$ of D into triangles (or tetrahedra in 3D) with sides $\mathcal{E}$ and nodes $\mathcal{N}$. The discretisation with conforming finite elements $V_h := P_p(\mathcal{T}) \cap V$ of degree $p \geq 1$ where

$$P_p(\mathcal{T}) := \{v \in L^2(D) \mid \forall T \in \mathcal{T}\ \ v|_T \text{ is polynomial of maximal degree } p\}$$

leads to a discrete solution $u_h \in V_h$ and its discrete flux $\sigma_h := a_0 \nabla u_h$ as an approximation of the exact flux $\sigma := a_0 \nabla u$. This solution is characterised by the Galerkin orthogonality property $r(V_h) = 0$ for the residual

$$r(v) := \int_D fv\, dx - \int_D \sigma_h \cdot \nabla v\, dx \quad \text{for all } v \in V.$$

It is well known that the dual norm of the residual is equivalent to the energy error for homogeneous Dirichlet boundary data, i.e.,

$$\|r\|_{V^*} := \sup_{v \in V} r(v)/\|v\|_V = \|u - u_h\|_{a_0} = \|a_0^{-1/2}(\sigma - \sigma_h)\|_{L^2(D)}.$$

1.3. **Inhomogeneous Dirichlet data.** In case of inhomogeneous Dirichlet boundary data, it holds

$$\|u - u_h\|^2_{a_0} = \|r\|^2_{V^*} + \inf_{\substack{w \in H^1(D) \\ w = u - u_h \text{ along } \partial D}} \|w\|^2_{a_0}.$$

Under the assumption $u_D \in H^1(\partial D) \cap H^2(\mathcal{E})$, the special choice of w from [5] leads to

$$0 \leq \inf_{\substack{w \in H^1(D) \\ w = u - u_h \text{ along } \partial D}} \|w\|_{a_0} \leq C \|h^{3/2} a_{0,\mathcal{T}} \partial^2 (u_D - u_h)/\partial s^2\|_{L^2(\partial D)},$$

with the local maximum diffusion coefficient $a_{0,\mathcal{T}}|_T := \operatorname{ess\,sup}_{x \in T} a_0(x)$ for all $T \in \mathcal{T}$ and a generic constant C that only depends on the shape of the triangles but not on their size. For meshes consisting of right isosceles triangles, [31] shows $C \leq 0.4980$.

2. Higher-order equilibration a posteriori error estimation

We start with a common ansatz for the design of equilibrated fluxes $q \in H(\operatorname{div}, D)$ which yields guaranteed upper bounds $\eta(q)$ for the error $u - u_h$ in the energy norm. Subsequently, global and local designs for equilibrated fluxes are explained. The local design is inspired by the lowest-order equilibration estimators of [18, 10, 8] and is generalised to finite element methods of arbitrary order $p \geq 1$. The suggested technique solves local problems and constructs equilibrated fluxes in the Brezzi-Douglas-Marini (BDM) finite element space [11] of order $k \geq p$ defined by

$$\mathrm{BDM}_k(\mathcal{T}) := \big\{ v_h \in P_k(\mathcal{T})^d : [v_h \cdot n_E] = 0 \text{ along all } E \in \mathcal{E} \big\}.$$

Its subspace of Raviart-Thomas (RT) finite element functions reads

$$\mathrm{RT}_{k-1}(\mathcal{T}) := \Big\{ v_h \in \mathrm{BDM}_k(\mathcal{T}) : \exists a \in P_{k-1}(\mathcal{T})^d, b \in P_{k-1}(\mathcal{T}),\ v_h(x) = a + bx \text{ a.e.} \Big\}.$$

In the following derivations, a piecewise L^2 projection operator for $f \in L^2(D)$ onto $P_{k-1}(\mathcal{T})$ is required which we denote by $\Pi_{k-1}(f)$.

2.1. **Equilibration ansatz.**

First, an integration by parts allows to introduce an arbitrary $q \in H(\operatorname{div}, D)$ into the residual

$$r(v) = \int_D (f + \operatorname{div} q) v \, dx + \int_D (q - \sigma_h) \cdot \nabla v \, dx \quad \text{for all } v \in V.$$

If $q \in H(\operatorname{div}, D)$ is equilibrated in the sense that $\int_T f + \operatorname{div} q \ dx = 0$ for all $T \in \mathcal{T}$, an elementwise Poincaré inequality gives, for any $T \in \mathcal{T}$,

$$\begin{aligned} \int_T (f + \operatorname{div} q) v \, dx &= \int_T a_{0,T}^{-1/2} (f + \operatorname{div} q) a_{0,T}^{1/2} (v - v_T) \, dx \\ &\leq \frac{1}{\pi} \|h_T a_{0,T}^{-1/2} (f + \operatorname{div} q)\|_{L^2(T)} \|v\|_V \end{aligned}$$

where $a_{0,T} := \operatorname{ess\,inf}_{x \in T} a_0(x)$ and $v_T := \int_T v \, dx/|T|$. Note that in 2D the factor $1/\pi$ can be replaced by the sharper Poincaré constant $1/j_{1,1}$ for triangles with the first positive root $j_{1,1}$ of the first Bessel function [27]. A Cauchy inequality in $\mathbb{R}^{|\mathcal{T}|}$ leads to

$$r(v) \ \leq \ \left(\sum_{T \in \mathcal{T}} \left(\frac{1}{\pi} \|h_T a_{0,T}^{-1/2} (f + \operatorname{div} q)\|_{L^2(T)} + \|a_0^{-1/2} (q - \sigma_h)\|_{L^2(T)} \right)^2 \right)^{1/2} \|v\|_V.$$

Hence, we may define the generic error estimator $\eta(q)$ for which holds

(2.1)
$$\|r\|_{V^*}^2 \leq \eta(q)^2 := \sum_{T\in\mathcal{T}} \left(\frac{1}{\pi} \|h_T a_{0,T}^{-1/2}(f + \operatorname{div} q)\|_{L^2(T)} + \|a_0^{-1/2}(q - \sigma_h)\|_{L^2(T)} \right)^2 .$$

It remains to design an equilibrated quantity q by global or local equilibration techniques.

2.2. **Global equilibration.** The global equilibration error estimator for any discrete space $Q(\mathcal{T}) \subset H(\operatorname{div}, D)$ computes the constrained minimiser

$$q = \operatorname{argmin}_{\tau\in Q(\mathcal{T})} \left\{ \|a_0^{-1/2}(\tau - \sigma_h)\|_{L^2(\Omega)} \;\middle|\; \operatorname{div}\tau + \Pi_{k-1} f = 0 \right\}.$$

Possible $H(\operatorname{div}, D)$-conforming choices for $Q(\mathcal{T})$ are Raviart-Thomas ($\mathrm{RT}_{k-1}(\mathcal{T})$) or Brezzi-Douglas-Marini ($\mathrm{BDM}_k(\mathcal{T})$) finite element spaces of any order $k \geq p$ for the given polynomial order p of the discrete method. See [9] for a proof that the efficiency of these global equilibration error estimators is robust with respect to p.

2.3. **Local equilibration.** The local equilibration error estimator solves local minimisation problems on the overlapping subtriangulations $\mathcal{T}(z) := \{T \in \mathcal{T} : z \in T\}$ for every node $z \in \mathcal{N}$ with adjacent sides $\mathcal{E}(z) := \{E \in \mathcal{E} : z \in E\}$, similar to the technique due to Destuynder and Métivet [18] or Braess [10, 8]. For the application to higher-order finite element methods with $\nabla u_h \in P_{p-1}(\mathcal{T})$, we design an equilibrated BDM function $q \in \mathrm{BDM}_k$ of order $k \geq p$.

To cope with nonconstant diffusion coefficients, the piecewise polynomial stress approximation

$$\widetilde{\sigma}_h|_T := \Pi_{k-1}\sigma_h$$

enters the constraints for the local minimisation problems

(2.2)
$$q_z = \operatorname{argmin}_{\tau\in P_k(\mathcal{T}(z))^d} \Big\{ \|a_0^{-1/2}\tau\|_{L^2(\omega_z)} \;\Big|\; \tau\cdot n = 0 \text{ on } \partial\omega_z \setminus \partial\Omega, \forall T \in \mathcal{T}(z),$$
$$\operatorname{div}\tau + \Pi_{k-1}(f\varphi_z) + \operatorname{div}(\widetilde{\sigma}_h)\varphi_z = 0 \;\&\; \forall E \in \mathcal{E}(z), [\tau\cdot n_E] = -\varphi_z[\widetilde{\sigma}_h\cdot n_E] \Big\}.$$

The well-posedness of this problem for interior nodes is connected to the Galerkin orthogonality

$$r(\varphi_z) = \int_D f\varphi_z - \sigma_h\cdot\nabla\varphi_z\,dx = \int_D \Pi_{k-1}(f\varphi_z) - \widetilde{\sigma}_h\cdot\nabla\varphi_z\,dx = 0 \quad \text{for all } z \in \mathcal{N}(D).$$

This, the chain rule and a piecewise integration by parts yields the consistency condition

$$\begin{aligned}\int_{\omega_z} \operatorname{div} q_z\,dx &= \sum_{E\in\mathcal{E}(z)} \int_E [q_z\cdot n_E]\,ds = -\sum_{E\in\mathcal{E}(z)} \int_E \varphi_z[\widetilde{\sigma}_h\cdot n_E]\,ds \\ &= -\int_{\omega_z} \operatorname{div}\widetilde{\sigma}_h\varphi_z + \widetilde{\sigma}_h\cdot\nabla\varphi_z\,dx - r(\varphi_z) \\ &= -\int_{\omega_z} \Pi_{k-1}(f\varphi_z) + \operatorname{div}(\widetilde{\sigma}_h)\varphi_z\,dx.\end{aligned}$$

With the partition of unity property $\sum_{z\in\mathcal{N}}\varphi_z \equiv 1$, it is easy to see that $q := \widetilde{\sigma}_h + \sum_{z\in\mathcal{N}} q_z \in \mathrm{BDM}_k(\mathcal{T})$ indeed satisfies $[q\cdot n_E] = 0$ for all $E \in \mathcal{E}$ and

$$\operatorname{div} q + \sum_{z\in\mathcal{N}(T)} \Pi_{k-1}(f\varphi_z) = \operatorname{div} q + \Pi_{k-1}(f) = 0.$$

Hence, q is a valid equilibrated quantity that allows for (2.1).

Remark 2.1. (a) Note, that $\widetilde{\sigma}_h - \sigma_h \equiv 0$ for $a_0 \in P_0(\mathcal{T})$.
(b) The ansatz space for the local minimisation problems can be reduced to broken Raviart-Thomas functions of order $k-1$ if the jump condition $[\tau \cdot n_E] = -\varphi_z[\widetilde{\sigma}_h \cdot n_E]$ is replaced by $[\tau \cdot n_E] = -\Pi_{k-1}(\varphi_z[\widetilde{\sigma}_h \cdot n_E])$. For $p = 1 = k$, this equals the condition in the equilibration error estimator from [18, 10, 8].
(c) The local equilibration error estimator $\eta(q)$ is equivalent to the classical residual error estimator

$$\eta(q)^2 \approx \sum_{T\in\mathcal{T}} \frac{h_T^2}{a_{0,T}} \Big(\|\Pi_{k-1}(f) + \operatorname{div}\sigma_h\|_{L^2(D)}^2 + \|f - \Pi_{k-1}(f)\|_{L^2(D)}^2 \Big) + \sum_{E\in\mathcal{E}} \frac{h_E}{a_{0,E}} \|[\sigma_h \cdot n_E]\|_{L^2(D)}^2.$$

A proof for the original Braess equilibration error estimator for $p = 1 = k$ and $a_0 \equiv 1$ can be found in [8, Theorem 9.5, p.184 f.]. It can easily be extended to higher order fluxes. For nonconstant coefficients $a_0 \notin P_0(\mathcal{T})$, the additional term $\|a_0^{-1/2}(\sigma_h - \Pi_{k-1}\sigma_h)\|_{L^2(D)}$ arises which is of higher order for $k > p$.
(d) For practical purposes, the conditions in (2.2) can be (weakly) enforced by penalisation with some sufficiently small $\varepsilon > 0$ in the functional

$$F(\tau) = \|\tau\|_{L^2(\omega_z)}^2 + \frac{1}{\varepsilon}\|\operatorname{div}\tau + \Pi_{p-1}(f\varphi_z) + \operatorname{div}(\widetilde{\sigma}_h)\varphi_z\|_{L^2(\omega_z)}^2 + \frac{1}{\varepsilon}\|[(\tau - \widetilde{\sigma}_h\varphi_z)\cdot n_E]_E\|_{L^2(\mathcal{E}(z))}^2 + \frac{1}{\varepsilon}\|\tau\cdot n_E\|_{L^2(\partial\omega_z\setminus\Gamma_D)}^2. \tag{2.3}$$

The discrete minimiser $\tau \in P_k(\mathcal{T}(z))^d$ of F is obtained by solving $a_\varepsilon(\tau, v) = \ell_\varepsilon(v)$ for all $v \in P_k(\mathcal{T}(z))^d$ with

$$\begin{aligned} a_\varepsilon(\tau, v) &:= \int_{\omega_z} a_0^{-1}\tau\cdot v\,dx + \frac{1}{\varepsilon}\int_{\omega_z}\operatorname{div}\tau\operatorname{div}v\,dx + \frac{1}{\varepsilon}\int_{\mathcal{E}(z)}[\tau\cdot n_E][v\cdot n_E]\,ds \\ &\quad + \frac{1}{\varepsilon}\int_{\mathcal{E}(\partial\omega_z)\setminus\mathcal{E}(\Gamma_D)}(\tau\cdot n_E)(v\cdot n_E)\,ds \qquad (2.4) \\ \ell_\varepsilon(v) &:= -\frac{1}{\varepsilon}\int_{\omega_z}(\Pi_{k-1}(f\varphi_z) + \operatorname{div}(\widetilde{\sigma}_h)\varphi_z)\operatorname{div}v\,dx - \frac{1}{\varepsilon}\int_{\mathcal{E}(z)}[\widetilde{\sigma}_h\cdot n_E][v\cdot n_E]\varphi_z\,ds. \end{aligned}$$

The limit for $\varepsilon \to 0$ is the (conforming) minimiser q_z.

2.4. **Numerical comparison.** Two numerical examples demonstrate the performance of the local equilibration error estimators for different orders $p = 1, 2, 3$. The mesh refinement is based on the common bulk criterion with some bulk parameter $\Theta \in (0, 1)$. For some estimator $\eta^2 = \sum_{T\in\mathcal{T}}\eta_T^2$ with local contributions η_T on each $T \in \mathcal{T}$, we assume a marking set $\mathcal{M} \subset \mathcal{T}$ of smallest cardinality such that

$$\sum_{T\in\mathcal{M}}\eta_T^2 \geq \Theta\sum_{T\in\mathcal{T}}\eta_T^2. \tag{2.5}$$

In the following experiments, the determination of $\mathcal{M}$ is performed with $\Theta = 0.5$ and the local contributions of the equilibration error estimators from (2.1) for several realisations of q. All exact energy errors and efficiency indices where computed with regard to a reference overkill solution.

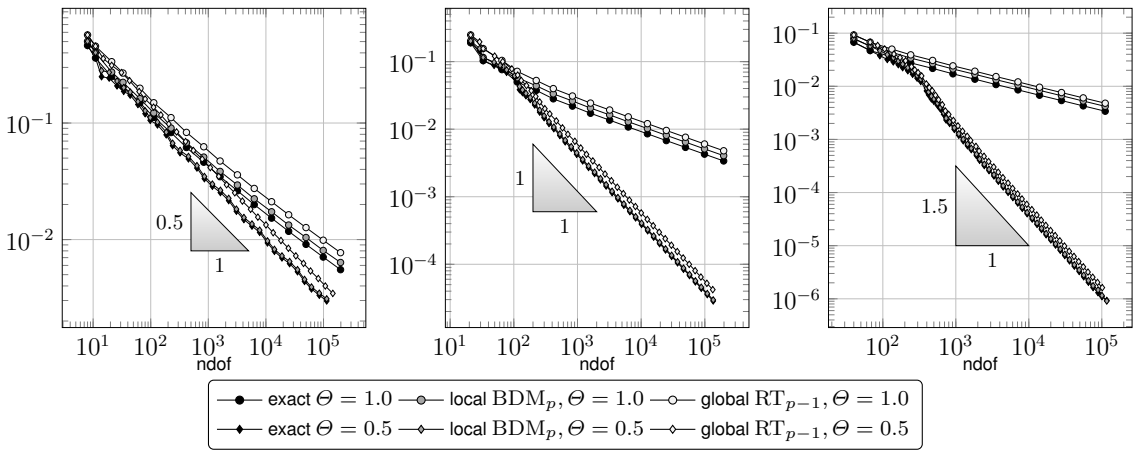

FIGURE 1. Convergence of the exact energy error and some error estimators for FEM of degree $p = 1$ (left), $p = 2$ (middle) and $p = 3$ (right) for uniform and adaptive mesh refinement versus the number of degrees of freedom (ndof) for the stationary diffusion problem on the L-shaped domain as detailed in Section 2.4.1.

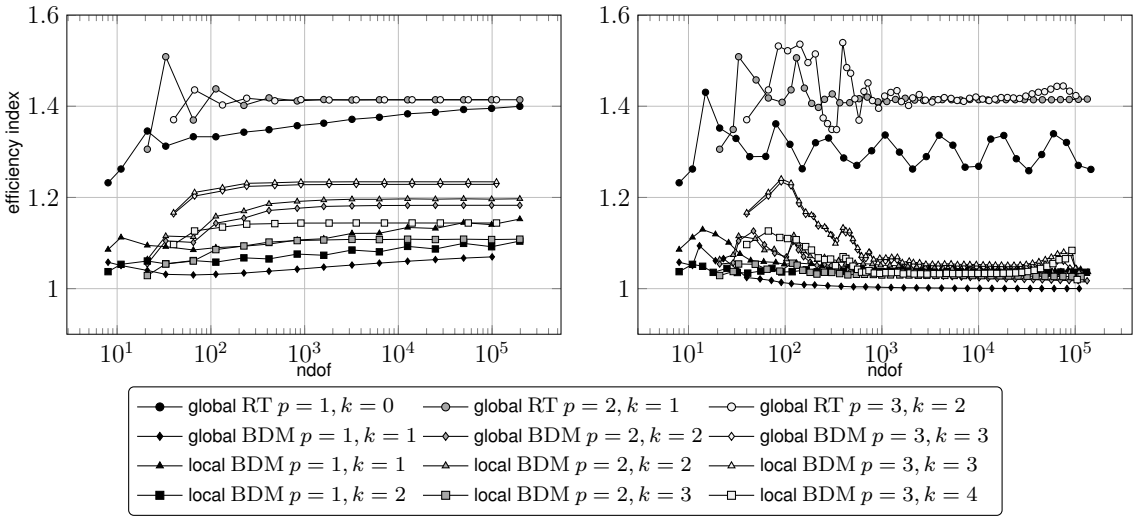

FIGURE 2. Efficiency indices of the local and global equilibration error estimators for different FEM degrees $p = 1, 2, 3$ and equilibration degrees k for uniform (left) and adaptive (right) mesh refinement for the stationary diffusion problem on the L-shaped domain as detailed in Section 2.4.1.

Further numerical examples in the context of PDE with stochastic data are discussed in Section 8.

2.4.1. *Example 1: Constant coefficient on L-shaped domain.* The first example considers equation (1.1) with homogeneous diffusion coefficient $a_0 \equiv 1$ and $f \equiv 1$ on the L-shaped domain $D = (-1, 1)^2 \setminus (0, 1) \times (-1, 0)$. It is well-known that the solution exhibits a singularity at the reentrant corner at $(0, 0)$ which should be resolved by a successive refinement in its vicinity. With this, the (otherwise reduced) optimal convergence rate is recovered. Figure 1 shows the convergence history of the exact energy error and the global and local equilibration error estimators for adaptive and uniform mesh refinement and polynomial degrees $p = 1, 2, 3$. The convergence

rates for the different polynomial degrees and adaptive mesh refinement are optimal, i.e. higher for larger p. With uniform refinement, we observe the same low decreased rate in all cases.

The plotted local equilibration error estimator with BDM functions and $k = p$ always yields a slightly better bound than the global equilibration with Raviart-Thomas functions of order $k = p-1$. Figure 2 shows the efficiency indices of these two estimators and further configurations. While the global error estimator with Raviart-Thomas functions attains efficiency indices around 1.4 for uniform mesh refinement, the efficiency indices of the local error estimators with BDM functions and $k = p$ are all below 1.2, very close to the global error estimator with BDM functions and $k = p$. The error estimators with local problems solved by BDM functions of order $k = p+1$ all lead to very good efficiency indices below 1.5. The results for adaptive mesh refinement are similar.

2.4.2. *Example 2: Inhomogeneous coefficient on unit square.* The second example considers equation (1.1) on the unit square $D = (0, 1)^2$ with inhomogeneous diffusion coefficient $a_0(x_1, x_2) = 3+\sin(7\pi x_1)+\sin(9\pi x_2)$ and f such that the homogeneous Dirichlet boundary conditions are satisfied. In this setup, the analytic solution is known and used for the evaluation of the error and the efficiency. Since a_0 is nonconstant, $\tilde{\sigma}_h \neq \sigma_h$ appears in the local equilibration estimator. Opposite to the first example, the solution in this experiment exhibits high regularity in the entire domain. Thus, the convergence rates for the polynomial degrees $p = 1, 2, 3$ shown in Figure 3 are optimal both for adaptive (top) and uniform (bottom) refinement.

In contrast to the first example, the efficiency indices of the global equilibration error estimator with Raviart-Thomas elements of order $k = p - 1$ and of the local equilibration error estimator with BDM element of order $k = p$ are not as good as in the first example. This nonoptimality seems to increase with the polynomial degree p and leads to efficiency indices of about 2.5 for $p = 1$, 10 for $p = 2$ and even more than 30 for $p = 3$ as depicted in Figure 4. However, the global equilibration error estimator with BDM elements of order $k = p$ and the local versions with order $k = p + 1$ asymptotically regain their very good efficiency indices from the first experiment. The cause for this behavior possibly is the highly oscillating diffusion coefficient. To perform the local equilibration, an approximation of the flux σ_h by $\widetilde{\sigma}_h = \Pi_k\sigma_h$ is introduced in the estimator and might cause additional errors and the degraded efficiency indices. With local ansatz spaces of order $k = p+1$ this additional error becomes less significant and decreases with higher order. Interestingly, the local equilibration error estimator with BDM functions of order $k = p + 1$ leads to significantly better efficiency indices than the global equilibration error estimator with BDM function of order $k = p$, especially on coarse meshes. Note that this is also the case in the first example, but only for $p > 1$.

3. Stochastic model problem

This section introduces the stochastic model problem which corresponds to (1.1) with stochastic coefficient a. It is formulated as a parametric PDE depending on a countable infinite set of parameters y which leads to the weak formulation of the problem, see [36] for a broader presentation.

3.1. **A parametric elliptic boundary value problem.** We assume some Lipschitz domain $D \subset \mathbb{R}^d$, a sequence of scalar parameters $y := (y_m)_{m\in\mathbb{N}}$ and some coefficient function a with

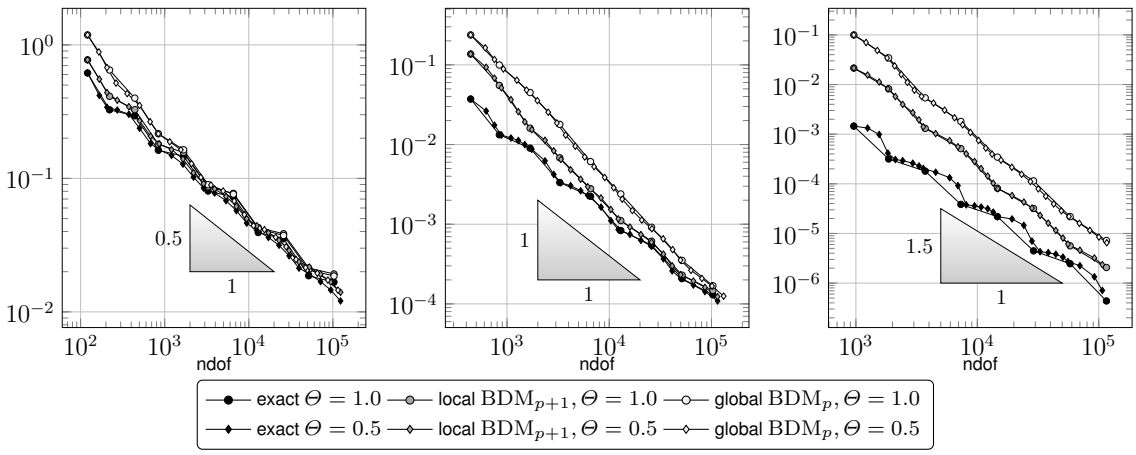

FIGURE 3. Convergence of the exact energy error and some error estimators for FEM of degree $p = 1$ (left), $p = 2$ (middle) and $p = 3$ (right) for uniform and adaptive mesh refinement versus the number of degrees of freedom (ndof) for the stationary diffusion problem on the unit square domain as detailed in Section 2.4.2.

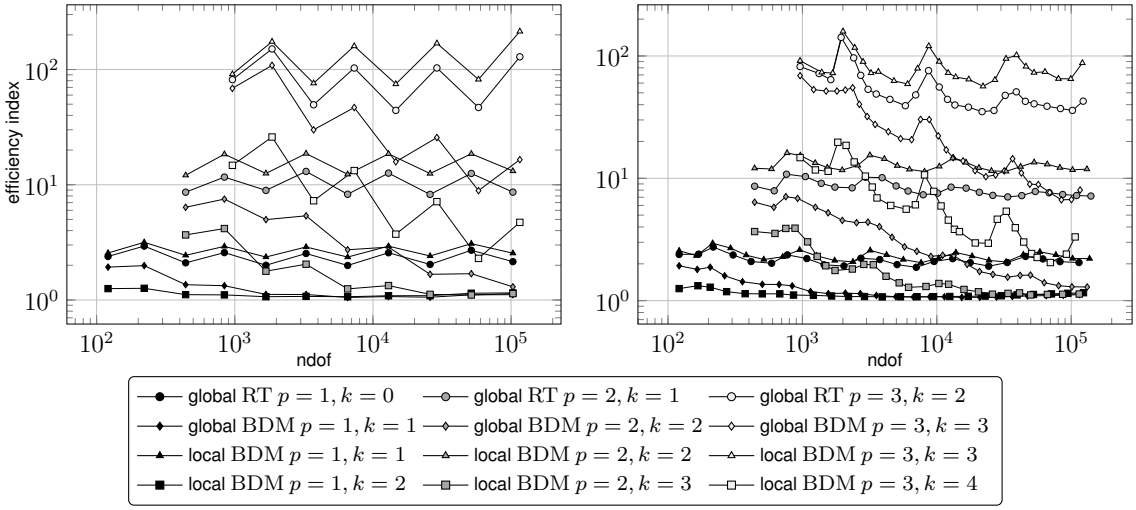

FIGURE 4. Efficiency indices of the local and global equilibration error estimators for different FEM degrees $p = 1, 2, 3$ and equilibration degrees k for uniform (left) and adaptive (right) mesh refinement for the stationary diffusion problem on unit square domain (bottom) as detailed in Section 2.4.2.

affine dependence on y with the representation

$$a(y, x) := a_0(x) + \sum_{m=1}^{\infty} y_m a_m(x), \quad x \in D. \tag{3.1}$$

This could e.g. be the Karhunen-Loève expansion of the random field a with random variables $(y_m)_{m\in\mathbb{N}}$. We then consider the parametric elliptic boundary value problem

$$-\nabla \cdot (a\nabla u) = f \text{ in } D, \qquad u = 0 \text{ on } \partial D. \tag{3.2}$$

We assume $y \in \Gamma := [-1,1]^\infty$, i.e., $|y_m| \le 1$, bounded first derivatives, i.e., $a_m \in W^{1,\infty}(D)$,

$$\operatorname*{ess\,inf}_{x\in D} a_0(x) > 0 \quad \text{and} \quad \sum_{m=1}^{\infty} \left\| \frac{a_m}{a_0} \right\|_{L^\infty(D)} \le \gamma < 1. \tag{3.3}$$

This implies convergence in (3.1) and positivity of a. With the operator A defined by

$$A(y) : H_0^1(D) \to H^{-1}(D), \quad v \mapsto \nabla \cdot (a \nabla v) \quad \text{for } y \in \Gamma, \tag{3.4}$$

equation (3.2) can be written as $A(y)u(y) = f$. Moreover, A can be expanded into an unconditionally convergent series in the function space of linear maps $\mathcal{L}(V, V^*)$ in the form

$$A(y) = A_0 + \sum_{m=1}^{\infty} y_m A_m \quad \text{for all } y \in \Gamma \tag{3.5}$$

where

$$A_m : H_0^1(D) \to H^{-1}(D), \quad v \mapsto \nabla \cdot (a_m \nabla v). \tag{3.6}$$

The assumptions regarding the coefficient a ensure uniform ellipticity and thus the unique solvability of (3.2).

3.2. **Weak formulation.** The weak formulation of (3.2) with respect to the parameter y requires a measure on the parameter domain Γ. We consider symmetric Borel measures which entails that the parameters y_m are independent and have symmetric distributions.

For each $m \in \mathbb{N}$, let π_m be the symmetric Borel probability measure of y_m on $[-1,1]$. The product measure

$$\pi := \bigotimes_{m=1}^{\infty} \pi_m \tag{3.7}$$

is a probability measure on Γ. The weak formulation results from the integration of (3.2) with respect to π, i.e.,

$$\int_\Gamma \langle A(y)u(y), v(y)\rangle d\pi(y) = \int_\Gamma \int_D f(x)v(y,x)dxd\pi(y) := F(v), \tag{3.8}$$

where $\langle \cdot, \cdot \rangle = \langle \cdot, \cdot \rangle_{V^*,V}$ denotes the usual duality pairing between a vector space and its dual. The left-hand side of (3.8) is a scalar product on $\mathcal{V} = L^2_\pi(\Gamma; V)$ for $w, v \in \mathcal{V}$,

$$(w,v)_{\mathcal{A}} := \int_\Gamma \langle A(y)w(y), v(y)\rangle d\pi(y) = \int_\Gamma \int_D a(y,x)\nabla w(y,x) \cdot \nabla v(y,x) dx d\pi(y) \tag{3.9}$$

which induces the energy norm $\|v\|^2_{\mathcal{A}} := (v,v)_{\mathcal{A}}$ for $v \in \mathcal{V}$. Moreover, the mean energy norm reads

$$\|v\|^2_{L^2_\pi(\Gamma;V)} := \int_\Gamma \int_D a_0 \nabla v \cdot \nabla v \; dx d\pi(y). \tag{3.10}$$

Existence and uniqueness of the solution u of (3.8) follow from the Riesz representation theorem. Moreover, u coincides with the solution of (3.2) for π-a.e. $y \in \Gamma$.

4. Stochastic Galerkin FEM

For the discretisation of the weak problem (3.8) with the stochastic Galerkin FEM, an orthonormal system of polynomials as a basis for the stochastic space is defined. Upon a selection of a (finite) active set Λ of stochastic modes, this leads to a semi-discretisation of the problem and a semi-discrete best-approximation u_Λ of u. The fully discrete system is obtained with the discretisation of the deterministic space by higher-order FEM. By this, the fully discrete Galerkin approximation u_N is obtained.

Let $\mathcal{F}$ be the set of finitely supported multi-indices

$$\mathcal{F} \coloneqq \{\mu \in \mathbb{N}_0^\infty \mid |\operatorname{supp}\mu| < \infty\} \tag{4.1}$$

where $\operatorname{supp}\mu \coloneqq \{m \in \mathbb{N} \mid \mu_m \neq 0\}$ and let $|\mu| \coloneqq \sum_{i\in\operatorname{supp}\mu} \mu_i$. For any subset $\Lambda \subset \mathcal{F}$, we define $\operatorname{supp}\Lambda \coloneqq \bigcup_{\mu\in\Lambda} \operatorname{supp}\mu \subset \mathbb{N}$. The infinite set

$$\partial\Lambda \coloneqq \{\nu \in \mathcal{F} \setminus \Lambda \mid \exists m \in \mathbb{N} : \nu - \epsilon_m \in \Lambda \vee \nu + \epsilon_m \in \Lambda\} \tag{4.2}$$

defines the boundary of Λ. Likewise, the active boundary of Λ is defined by

$$\partial^\circ\Lambda \coloneqq \{\nu \in \mathcal{F} \setminus \Lambda \mid \exists m \in \operatorname{supp}\Lambda : \nu - \epsilon_m \in \Lambda \vee \nu + \epsilon_m \in \Lambda\} \tag{4.3}$$

which is a finite set in case that $|\Lambda| < \infty$.

4.1. **Tensor product orthogonal polynomial basis.** For each $m \in \mathbb{N}$, let $(P_n^m)_{m=0}^\infty$ denote an orthogonal polynomial basis of $L^2_{\pi_m}([-1,1])$ of degree $\deg(P_n^m) = n$. Due to symmetry of π_m, such bases satisfy a recursion of the form

$$\beta_n^m P_n^m(y_m) = y_m P_{n-1}^m(y_m) - \beta_{n-1}^m P_{n-2}^m(y_m) \quad \text{for } n \geq 1 \tag{4.4}$$

with $P_0^m \coloneqq 1$ and $\beta_0^m \coloneqq 0$. We assume a uniform distribution $d\pi_m(y_m) = \frac{1}{2}dy_m$ in which case the $(P_n^m)_{n=0}^\infty$ are Legendre polynomials and $\beta_n^m = (4-n^{-2})^{-1/2}$.

An orthogonal basis of $L^2_\pi(\Gamma)$ is obtained by tensorisation of the univariate polynomials. For any $\mu \in \mathcal{F}$, the tensor product polynomial $P_\mu \coloneqq \bigotimes_{m=1}^\infty P_{\mu_m}^m$ in $y \in \Gamma$ is expressed as the finite product

$$P_\mu(y) = \prod_{m=1}^\infty P_{\mu_m}^m(y_m) = \prod_{m\in\operatorname{supp}\mu} P_{\mu_m}^m(y_m). \tag{4.5}$$

Recursion (4.4) implies

$$y_m P_\mu(y) = \beta_{\mu_m+1}^m P_{\mu+\epsilon_m}(y) + \beta_{\mu_m}^m P_{\mu-\epsilon_m}(y) \tag{4.6}$$

with the Kronecker sequence $\epsilon_m \coloneqq (\delta_{mn})_{n=1}^\infty$. Moreover, we set $P_\mu \coloneqq 0$ for $\mu_m < 0$. The family of polynomials $(P_\mu)_{\mu\in\mathcal{F}}$ forms an orthonormal basis of $L^2_\pi(\Gamma)$, see [36].

4.2. **Stochastic discretisation.** The solution u of (3.8) in the basis $(P_\mu)_{\mu\in\mathcal{F}}$ of $L^2_\pi(\Gamma)$ with coefficients $u_\mu \in V$ for $\mu \in \mathcal{F}$ has the $L^2_\pi(\Gamma;V)$ convergent expansion

$$u(y,x) = \sum_{\mu\in\mathcal{F}} u_\mu(x) P_\mu(y). \tag{4.7}$$

The sequence of coefficients $(u_\mu)_{\mu\in\mathcal{F}} \in \ell^2(\mathcal{F};V)$ is determined by the infinite coupled system

$$A_0 u_\mu + \sum_{m=1}^{\infty} A_m \left(\beta^m_{\mu_m+1} u_{\mu+\epsilon_m} + \beta^m_{\mu_m} u_{\mu-\epsilon_m}\right) = f\delta_{\mu 0} \quad \text{for } \mu \in \mathcal{F}. \tag{4.8}$$

For any subset $\Lambda \subset \mathcal{F}$, we define the (stochastically) semi-discrete space

$$\mathcal{V}(\Lambda) := \left\{ v_\Lambda(y,x) = \sum_{\mu\in\mathcal{F}} v_{\Lambda,\mu}(x) P_\mu(y) \mid v_{\Lambda,\mu} \in V \;\forall\; \mu \in \Lambda \right\} \subset \mathcal{V} := L^2_\pi(\Gamma;V). \tag{4.9}$$

The Galerkin projection of u onto $\mathcal{V}(\Lambda)$ is the unique $u_\Lambda \in \mathcal{V}(\Lambda)$ which satisfies

$$(u_\Lambda, v)_{\mathcal{A}} = F(v) \quad \text{for all } v \in \mathcal{V}(\Lambda). \tag{4.10}$$

If Λ is finite, the sequence of coefficients $(u_{\Lambda,\mu})_{\mu\in\mathcal{F}} \in V^\Lambda := \prod_{\mu\in\mathcal{F}} V$ of u_Λ is determined by the finite system

$$A_0 u_{\Lambda,\mu} + \sum_{m=1}^{\infty} A_m \left(\beta^m_{\mu_m+1} u_{\Lambda,\mu+\epsilon_m} + \beta^m_{\mu_m} u_{\Lambda,\mu-\epsilon_m}\right) = f\delta_{\mu 0} \quad \text{for } \mu \in \Lambda \tag{4.11}$$

where we set $u_{\Lambda,\nu} = 0$ for $\nu \in \mathcal{F}\setminus\Lambda$. Note that all terms in the sum (4.11) vanish for $m \in \mathbb{N} \setminus \operatorname{supp}\Lambda$.

4.3. **Deterministic discretisation.** We discretise the deterministic space V by a conforming finite element space $V_p(\mathcal{T}) \subset V$ of degree p on some simplicial mesh $\mathcal{T}$ of D. Then, the fully discrete space is defined by

$$\mathcal{V}_p(\Lambda;\mathcal{T}) := \left\{ v_N(y,x) = \sum_{\mu\in\mathcal{F}} v_{N,\mu}(x) P_\mu(y) \mid \forall\; \mu \in \Lambda,\; v_{N,\mu} \in V_p(\mathcal{T}) \right\} \subset \mathcal{V}(\Lambda). \tag{4.12}$$

Similar to (4.10), the Galerkin projection of u is the unique $u_N \in \mathcal{V}_p(\Lambda;\mathcal{T})$ which satisfies

$$(u_N, v)_{\mathcal{A}} = F(v) \quad \text{for all } v \in \mathcal{V}_p(\Lambda;\mathcal{T}). \tag{4.13}$$

The sequence of coefficients $(u_{N,\mu})_{\mu\in\Lambda} \in V_p(\mathcal{T})^\Lambda = \prod_{\mu\in\Lambda} V_p(\mathcal{T})$ for $\mu \in \Lambda$ is determined by

$$\int_D (A_0 u_{N,\mu}) v \, dx + \sum_{m=1}^{\infty} \int_D A_m \left(\beta^m_{\mu_m+1} u_{\mu+\epsilon_m} + \beta^m_{\mu_m} u_{\mu-\epsilon_m}\right) v \, dx = \int_D f\delta_{\mu 0} v \, dx \tag{4.14}$$

for all $v \in V_p(\mathcal{T})$. Note that we set $u_{N,\nu} = 0$ for $\nu \in \mathcal{F}\setminus\Lambda$ as before.

5. Expansion of the stochastic residual

In this section we are concerned with the definition of the stochastic residual with respect to some discrete function $w_N \in \mathcal{V}_p(\Lambda;\mathcal{T})$. In particular, an appropriate splitting and decomposition enables the derivation of mode-local residual contributions which can then be bounded by the error estimator derived in Section 6.

For any $w_N \in \mathcal{V}_p(\Lambda;\mathcal{T})$ and $v \in \mathcal{V}$, the residual $\mathcal{R}(w_\Lambda) \in L^2_\pi(\Gamma;V^*)$ is defined with respect to the exact solution u by

$$\begin{aligned}\mathcal{R}(w_N)(v) &:= (u - w_N, v)_{\mathcal{A}} = F(v) - (w_N, v)_{\mathcal{A}} \\ &= \int_\Gamma \int_D \left(fv - a\nabla w_N \cdot \nabla v\right)\, dx d\pi.\end{aligned}$$

For $\nu \in \Lambda$, the discrete stochastic stress reads

$$\sigma_\nu(w_N) := a_0 \nabla w_{N,\nu} + \sum_{m=1}^{\infty} a_m \nabla \left(\beta^m_{\nu_m+1} w_{N,\nu+\epsilon_m} + \beta^m_{\nu_m} w_{N,\nu-\epsilon_m}\right)$$

and defines the local residuals $r_\nu(w_N) \in L^2_\pi(\Gamma;V^*)$ which are the projections of $\mathcal{R}$ onto the polynomial basis $\{P_\nu\}_{\nu\in\mathcal{F}}$ in the sense

$$r_\nu(w_N)(v_\nu) = \mathcal{R}(w_N)(v_\nu P_\nu) \tag{5.1}$$

$$= \int_D f\delta_{\nu 0} v_\nu - \sigma_\nu(w_N)\cdot\nabla v_\nu\, dx \quad \text{for all } v_\nu \in V. \tag{5.2}$$

Given any $v = \sum_{\nu\in\mathcal{F}} v_\nu P_\nu \in L^2_\pi(\Gamma;V)$, these local residuals spawn the global residual in the sense that

$$\begin{aligned}\mathcal{R}(w_N)(v) &= \sum_{\nu\in\mathcal{F}} \int_\Gamma P_\nu\, d\pi \int_D f\delta_{\nu 0} v - \sigma(w_N)_\nu \cdot \nabla v\, dx \\ &= \sum_{\nu,\mu\in\mathcal{F}} \int_\Gamma P_\nu P_\mu\, d\pi \int_D f\delta_{\nu 0} v_\nu - \sigma(w_N)_\mu \cdot \nabla v_\nu\, dx \\ &= \sum_{\nu\in\mathcal{F}} r_\nu(w_N)(v_\nu).\end{aligned}$$

A consequence is the Parseval identity

$$\|\mathcal{R}(w_N)\|^2_{L^2_\pi(\Gamma;V^*)} = \sum_{\nu\in\mathcal{F}} \|r_\nu(w_N)\|^2_{V^*} \tag{5.3}$$

which holds with the dual norms

$$\|\mathcal{R}(w_\Lambda)\|^2_{L^2_\pi(\Gamma;V^*)} := \sup_{v\in L^2_\pi(\Gamma;V)} \mathcal{R}(w_N)(v)/\|v\|_{L^2_\pi(\Gamma;V)}$$

and

$$\|r_\nu(w_N)\|_{V^*} := \sup_{v\in V} r_\nu(w_N)(v)/\|v\|_V.$$

Remark 5.1 (Explicit derivation of (5.3)). Let $u^* \in L^2_\pi(\Gamma;V)$ and $u^*_\nu \in V$ be the Riesz representations of $\mathcal{R}(w_N)$ and $r_\nu(w_N)$ in the sense that

$$\mathcal{R}(w_N)(v) = (u^*, v)_{L^2_\pi(\Gamma;V)} \quad \text{for all } v \in L^2_\pi(\Gamma;V)$$

and

$$r_\nu(w_N)(v_\nu) = (u^*_\nu, v_\nu)_V \quad \text{for all } v_\nu \in V.$$

Thus, $\|u^*\|_{L^2_\pi(\Gamma;V)} = \|\mathcal{R}(w_N)\|_{L^2_\pi(\Gamma;V^*)}$ and $\|u^*_\nu\|_{L^2(V)} = \|r_\nu(w_N)\|_{V^*}$. Due to (5.1) and the equality $\|v\|^2_{L^2_\pi(\Gamma;V)} = \sum_{\nu\in\mathcal{F}}\|v_\nu\|^2_V$ for any $v = \sum_{\nu\in\mathcal{F}} v_\nu P_\nu \in L^2_\pi(\Gamma;V)$, for $\nu \in \mathcal{F}$ it holds

$$\begin{aligned}(u^*_\nu, v_\nu)_V = r_\nu(v_\nu) = \mathcal{R}(v_\nu P_\nu) = (u^*, v_\nu P_\nu)_{L^2_\pi(\Gamma;V)} &= \sum_{\mu\in\mathcal{F}}((u^*)_\mu P_\mu, v_\nu P_\nu)_{L^2_\pi(\Gamma;V)}\\ &= ((u^*)_\nu, v_\nu)_V.\end{aligned}$$

Hence, $u^*_\nu = (u^*)_\nu$ and so $\|u^*_\nu\|^2_V = \|(u^*)_\nu\|^2_V$. It follows that

$$\begin{aligned}\|\mathcal{R}(w_N)\|^2_{L^2_\pi(\Gamma;V^*)} = (u^*,u^*)_{L^2_\pi(\Gamma;V)} = \sum_{\nu\in\mathcal{F}}\|(u^*)_\nu\|^2_V &= \sum_{\nu\in\mathcal{F}}\|u^*_\nu\|^2_V\\ &= \sum_{\nu\in\mathcal{F}}\|r_\nu(w_N)\|^2_{V^*}.\end{aligned}$$

In this way, the total energy error of the partial stochastic problems can be related to the energy errors of the partial solutions $u^*_\nu \in V$ (for every $\nu \in \mathcal{F}$) that solve the Poisson problems according to (4.14). This proves (5.3).

For any $\Xi \subset \mathcal{F}$ and $v \in L^2_\pi(\Gamma;V)$, we set $R_\Xi(w_N)(v) := \sum_{\nu\in\Xi} r_\nu(w_N)(v_\nu P_\nu)$. Since $r_\nu(w_N)$ vanishes for $\nu \in \mathcal{F}\setminus(\Lambda\cup\partial\Lambda)$, it holds the decomposition

$$\mathcal{R}(w_N) = \mathcal{R}_\Lambda(w_N) + \mathcal{R}_{\partial\Lambda}(w_N). \tag{5.4}$$

Due to orthogonality, this yields the identity

$$\|\mathcal{R}(w_N)\|^2_{L^2_\pi(\Gamma;V^*)} = \|\mathcal{R}_\Lambda(w_N)\|^2_{L^2_\pi(\Gamma;V^*)} + \|\mathcal{R}_{\partial\Lambda}(w_N)\|^2_{L^2_\pi(\Gamma;V^*)}. \tag{5.5}$$

6. Residual based equilibration error estimation for the stochastic problem

In this section, we derive guaranteed upper error bounds for the stochastic error $u - w_N$, in particular for the discrete best approximation $u_N \in \mathcal{V}_p(\Lambda;\mathcal{T})$ of u defined by (4.13). This is established by the equivalence of the energy norm $\|\cdot\|_\mathcal{A}$ and the $L^2_\pi(\Gamma;V)$ norm, namely

$$(1-\gamma)\|v\|^2_{L^2_\pi(\Gamma;V)} \le \|v\|^2_\mathcal{A} \le (1+\gamma)\|v\|^2_{L^2_\pi(\Gamma;V)} \tag{6.1}$$

due to (3.3), see [25] for the derivation. Hence, by the Riesz representation theorem in $L^2_\pi(\Gamma;V^*)$, for any $w_N \in \mathcal{V}_p(\Lambda;\mathcal{T})$ it holds

$$\|u - w_N\|_\mathcal{A} = \sup_{v\in L^2_\pi(\Gamma;V)} \frac{\int_D \mathcal{A}(u-w_N)(v)\,dx}{\|v\|_\mathcal{A}} \le \frac{1}{\sqrt{1-\gamma}}\|\mathcal{R}(w_N)\|_{L^2_\pi(\Gamma;V^*)}. \tag{6.2}$$

It thus is necessary to devise bounds for the operator norm of the stochastic residual $\|\mathcal{R}(w_N)\|_{L^2_\pi(\Gamma;V^*)}$ for which we make use of the splitting (5.5) into the approximation part of the residual $\|\mathcal{R}_\Lambda(w_N)\|^2_{L^2_\pi(\Gamma;V^*)}$ and the stochastic tail $\|\mathcal{R}_{\partial\Lambda}(w_N)\|_{L^2_\pi(\Gamma;V^*)}$.

6.1. **Upper bounds for the approximation residual.**

The upper bound for the approximation part of the residual is based on the equilibration error estimators from Section 2 for the dual norms of the residual components $\|r_\nu(w_N)\|_{V^*}$ of (5.1). For some $w_N \in \mathcal{V}_p(\Lambda;\mathcal{T})$, the following lemma defines the error estimator $\eta(\Lambda, q)$ with respect to an equilibrated flux $q(w_N) = (q_\nu(w_{N,\nu}))_{\nu\in\Lambda}$.

Lemma 6.1. *Given $q_\nu \in H(\operatorname{div}, D)$ with $\int_T f\delta_{\nu 0} + \operatorname{div} q_\nu \, dx = 0$ for all $T \in \mathcal{T}$ and all $\nu \in \Lambda$, it holds*

$$\|\mathcal{R}_\Lambda(w_N)\|^2_{L^2_\pi(\Gamma;V^*)} \le \eta(\Lambda, q(w_N))^2 := \sum_{\nu\in\Lambda} \eta_\nu(q_\nu)^2. \tag{6.3}$$

Proof. This is a direct consequence of Parseval's identity (5.3) and (2.1). □

Remark 6.2. For $w_N = u_N$ from (4.13), each local residual enjoys the Galerkin orthogonality property $r_\nu(u_N)(V_p(\mathcal{T})) = 0$ which allows to estimate $\|r_\nu(w_N)\|_{V^*}$ by all kinds of known error estimators for Poisson problems. Further details can be found in [19, 20]. In particular, the local equilibration error estimators from Section 2 can be used. For $w_N \neq u_N$ without the local Galerkin orthogonality, modifications beyond the scope of this paper are in order to ensure the solvability of the local problems (2.2). The global equilibration error estimators can be used for arbitrary w_N.

6.2. **Upper bounds for the tail of the residual.** The stochastic tail error resulting from the selection of a finite active set $\Lambda \subset \mathcal{F}$ is represented by the tail residual $\mathcal{R}_{\partial\Lambda}$. For some $w_N \in \mathcal{V}_p(\Lambda;\mathcal{T})$ and $\nu \in \partial\Lambda$, we define

$$\zeta_\nu(w_N) := \sum_{m=1}^{\infty} \left\| \frac{a_m}{a_0} \right\|_{L^\infty(D)} \left(\beta^m_{\nu_m+1} \|w_{N,\nu+\epsilon_m}\|_V + \beta^m_{\nu_m} \|w_{N,\nu-\epsilon_m}\|_V \right). \tag{6.4}$$

Note that only terms for $\nu \pm \epsilon_m$ with $m \in \operatorname{supp}\Lambda$ do not vanish. The sum in (6.4) thus is finite. For any $\Delta \subset \partial\Lambda$, let

$$\zeta(w_N, \Delta) := \left(\sum_{\nu\in\Delta} \zeta_\nu(w_N)^2 \right)^{1/2}. \tag{6.5}$$

Lemma 6.3 ([20] Lem. 3.4)**.** *If $0 \in \Lambda$, for any $w_N \in \mathcal{V}_p(\Lambda;\mathcal{T})$ it holds*

$$\|\mathcal{R}_{\partial\Lambda}(w_N)\|_{L^2_\pi(\Gamma;V^*)} \le \zeta(w_N, \partial\Lambda). \tag{6.6}$$

Parseval's identity yields $\|\mathcal{R}_{\partial\Lambda}(w_N)\|^2_{L^2_\pi(\Gamma;V^*)} = \sum_{\nu\in\partial\Lambda} \|r_\nu(w_N)\|^2_{V^*}$. The indicator $\zeta(w_N, \partial\Lambda)$ is defined as an infinite sum in (6.5), for $\nu \in \partial\Lambda \setminus \partial^\circ\Lambda$ and it holds

$$\zeta_\nu(w_N) = \left\| \frac{a_m}{a_0} \right\|_{L^\infty(D)} \beta^m_1 \|w_{N,\mu}\|_V. \tag{6.7}$$

Summing over all inactive dimensions not in $\operatorname{supp}\Lambda$ leads to the error indicator

$$\bar\zeta_\mu(w_N, \Lambda) := \|w_{N,\mu}\|_V \left(\sum_{m\in\mathbb{N}\setminus\operatorname{supp}\Lambda} \left(\left\| \frac{a_m}{a_0} \right\|_{L^\infty(D)} \beta^m_1 \right)^2 \right)^{1/2} \quad \text{for } \mu \in \Lambda. \tag{6.8}$$

The terms in the sum are independent of w_N and μ. We assume that this infinite sum can be evaluated. Hence, $\zeta(w_N, \partial\Lambda)$ reads

$$\zeta(w_N, \partial\Lambda)^2 = \sum_{\nu\in\partial^\circ\Lambda} \zeta_\nu(w_N)^2 + \sum_{\mu\in\Lambda} \bar\zeta_\mu(w_N, \Lambda)^2. \tag{6.9}$$

6.3. **The complete upper bound.** The combination of the approximation residual error estimator $\eta(\Lambda, q(w_N))$ of Lemma 6.1 and the tail error estimator $\zeta(w_N, \partial\Lambda)$ of Lemma 6.3 yields the total error estimator $\eta_{\mathcal{A}}$.

Corollary 6.4. *For any $w_N \in \mathcal{V}_p(\Lambda;\mathcal{T})$, it holds*

$$\|u - w_N\|_{\mathcal{A}} \leq \eta_{\mathcal{A}} := \frac{1}{\sqrt{1-\gamma}} \left(\eta(\Lambda, q(w_N))^2 + \zeta(w_N, \partial\Lambda)^2\right)^{1/2}.$$

7. ADAPTIVE ALGORITHM

The adaptive algorithm described in this section is reminiscent of the algorithms presented in [20, 19] to which we refer for further details. In the following, we identify functional modules which encapsulate different aspects of the adaptive algorithm. Given some mesh $\mathcal{T}$, a finite set $\Lambda \subset \mathcal{F}$ including 0 and a fixed polynomial degree p, we assume that the Galerkin projection $u_N \in \mathcal{V}_p(\Lambda, \mathcal{T})$ of (4.13) is obtained by a function

$$u_N \leftarrow \mathtt{Solve}[\Lambda, \mathcal{T}].$$

The error indicators of Section 6 are computed by the methods

$$\begin{aligned}(\eta_T(u_N, \Lambda))_{T\in\mathcal{T}}, \eta(u_N, \Lambda, \mathcal{T}) &\leftarrow \mathtt{Estimate}_x[u_N, \Lambda, \mathcal{T}],\\ (\zeta_\nu(u_N))_{\nu\in\partial^\circ\Lambda}, \zeta(u_N, \partial\Lambda), (\|u_{N,\mu}\|_V)_{\mu\in\Lambda} &\leftarrow \mathtt{Estimate}_y[u_N, \Lambda].\end{aligned}$$

With these, a separate marking of elements of the mesh $\mathcal{T}$ and of modes of the inactive boundary $\partial^\circ\Lambda \subset \mathcal{F} \setminus \Lambda$ of Λ is carried out by the functions

$$\begin{aligned}\mathcal{M} &\leftarrow \mathtt{Mark}_x[\vartheta_x, (\eta_T(u_N, \Lambda))_{T\in\mathcal{T}}, \eta(u_N, \Lambda, \mathcal{T})],\\ \Delta &\leftarrow \mathtt{Mark}_y[\vartheta_y, (\zeta_\nu(u_N))_{\nu\in\partial^\circ\Lambda}, \zeta(u_N, \partial\Lambda), (\|u_{N,\mu}\|_V)_{\mu\in\Lambda}]\end{aligned}$$

with refinement parameters $0 < \vartheta_x, \vartheta_y < 1$. $\mathtt{Refine}_x$ is analog to the deterministic refinement (2.5) and details about the procedure $\mathtt{Refine}_y$ can be found in [20, Sec. 5.2]. The obtained smallest sets $\mathcal{M} \subset \mathcal{T}$ and $\Delta \subset \partial\Lambda$ satisfy the Dörfler property, i.e.,

$$\eta(u_N, \Lambda, \mathcal{M}) \geq \vartheta_x \eta(u_N, \Lambda, \mathcal{T}) \quad \text{and} \quad \zeta(u_N, \Delta) \geq \vartheta_y \zeta(u_N, \partial\Lambda).$$

With these marking sets, the following methods produce a refined regular mesh $\mathcal{T}^*$ and an enlarged active set Λ^*, namely,

$$\mathcal{T}^* \leftarrow \mathtt{Refine}_x[\mathcal{T}, \mathcal{M}] \quad \text{and} \quad \Lambda^* \leftarrow \mathtt{Refine}_y[\Lambda, \Delta].$$

In our case, $\Lambda^* = \Lambda \cup \Delta$ but other choices are possible. A single iteration step of an adaptive algorithm which returns either a refined $\mathcal{T}^*$ or Λ^* is given by the function $\mathtt{ASGFEM}$. For numerical simulations as performed in Section 8, this function has to be called iteratively until either a defined error bound threshold or a maximum problem size is reached.

Remark 7.1. Since the employed spatial equilibration error estimator η is equivalent to the residual based error estimator used in [20], the convergence and optimality results shown there directly carry over to the error estimator presented here.

$\mathcal{T}^*, \Lambda^* \leftarrow \texttt{ASGFEM}[\Lambda, \mathcal{T}, \vartheta_x, \vartheta_y]$

$u_N \leftarrow \texttt{Solve}[\Lambda, \mathcal{T}]$
$(\zeta_\nu)_{\nu\in\partial^\circ\Lambda}, \zeta, (\|u_{N,\mu}\|_V)_{\mu\in\Lambda} \leftarrow \texttt{Estimate}_y[u_N, \Lambda]$
$(\eta_T)_{T\in\mathcal{T}}, \eta \leftarrow \texttt{Estimate}_x[u_N, \Lambda, \mathcal{T}]$
if $\eta \geq \zeta$ **then**
  $\mathcal{M} \leftarrow \texttt{Mark}_x[\vartheta_x, (\eta_T)_{T\in\mathcal{T}}, \eta]$
  $\mathcal{T}^* \leftarrow \texttt{Refine}_x[\mathcal{T}, \mathcal{M}]$
else
  $\Delta \leftarrow \texttt{Mark}_y[\vartheta_y, (\zeta_\nu)_{\nu\in\partial^*\Lambda}, \zeta, (\|u_{N,\mu}\|_V)_{\mu\in\Lambda}]$
  $\Lambda^* \leftarrow \texttt{Refine}_y[\Lambda, \Delta]$

8. Implementation and numerical examples

This section is devoted to the numerical assessment of the proposed a posteriori error estimator. We employ the global mixed error estimator with BDM functions of Section 2.2 since our implementation for this estimator is in fact the most efficient (regarding computation time and also accuracy) with the same polynomial degree as the FEM space. A local error estimator would only slightly increase the over-estimation of the error as illustrated in the deterministic case in Section 2.4. The adaptive algorithm of Section 7 is implemented with the open source framework ALEA [21] which has already been used for the ASGFEM presented in [19, 20]. For the evaluation of the stochastic energy error of the numerical solution, we employ Monte-Carlo sampling based on a realisation-wise reference solution as described in Section 8.1. Subsequently, the performance of the new exact error estimator with regard to some benchmark problems on the square and the L-shaped domain as in [19, 20] is examined in Section 8.2.

8.1. **Evaluation of the error.** For experimental verification of the reliability of the error estimator, the error of the parametric solution is computed by Monte Carlo simulations. For this, a set of M independent realizations $\{y^{(i)}\}_{i=1}^M$ of the stochastic parameters is determined. The $y_m^{(i)}$ are sampled according to the probability measure π_m of the random variable y_m. The mean-square error e of the parametric SGFEM solution $u_N \in \mathcal{V}_p(\Lambda, \mathcal{T})$ is approximated by a Monte Carlo sample average

$$\|e\|_V^2 = \int_\Gamma \|u(y) - u_N(y)\|_V^2 \, d\pi(y) \approx \frac{1}{M}\sum_{i=1}^M \|\tilde{u}(y^{(i)}) - u_N(y^{(i)})\|_V^2 \,. \tag{8.1}$$

Note that the sampled solutions $\tilde{u}(y^{(i)})$ are approximations of the exact $u(y^{(i)}) = A^{-1}(y^{(i)})f$ since the differential operator is discretised on a fine reference mesh which is obtained by another uniform refinement of the adapted mesh generated from the SGFEM discretisation of the final iteration. Moreover, the truncated expansion (3.1) of the random field $a(y, x)$ is expanded by the trailing largest 200 terms which are not considered by the best approximate parametric solution. We choose $M = 150$ for the Monte Carlo sampling of the reference error (8.1) which proved to be sufficient to assess the reliability of the error estimator.

8.2. **The stochastic diffusion problem.** We examine numerical simulations for the stationary diffusion problem (3.2) in a plane, polygonal domain $D \subset \mathbb{R}^2$. As in [19, 20], the expansion

coefficients of the stochastic field (3.1) are given by

$$a_m(x) := \alpha_m \cos(2\pi\beta_1(m)x_1)\cos(2\pi\beta_2(m)x_2) \tag{8.2}$$

where α_m is of the form $\bar{\alpha}m^{-\tilde{\sigma}}$ with $\tilde{\sigma} > 1$ and some $0 < \bar{\alpha} < 1/\zeta(\tilde{\sigma})$ with the Riemann zeta function ζ. Then, (3.3) holds with $\gamma = \bar{\alpha}\zeta(\tilde{\sigma})$. Moreover,

$$\beta_1(m) = m - k(m)(k(m)+1)/2 \quad \text{and} \quad \beta_2(m) = k(m) - \beta_1(m) \tag{8.3}$$

with $k(m) = \lfloor -1/2 + \sqrt{1/4 + 2m} \rfloor$, i.e., the coefficient functions a_m enumerate all planar Fourier sine modes in increasing total order. To illustrate the influence which the stochastic coefficient plays in the adaptive algorithm, we examine the expansion with slow and fast decay of α_m, setting $\tilde{\sigma}$ in (8.2) to either 2 or 4. The computations are carried out with conforming FEM spaces of polynomial degrees 1, 2 and 3. For the adaptive algorithm ASGFEM of Section 7, the marking parameters are $\vartheta_x = \vartheta_y = 1/2$. The initial mesh $\mathcal{T}_0$ for newly activated $\mu \in \mathcal{F} \setminus \Lambda$ and the quadrature rule with exact integration of polynomials up to degree 15 are such that the solutions with respect to the oscillating coefficients a_m are computed with good accuracy.

8.2.1. *Square domain.* The first example is the stationary diffusion equation (3.2) on the unit square $D = (0,1)^2$ with homogeneous Dirichlet boundary conditions and with right-hand side $f \equiv 1$. The results of the adaptive algorithm ASGFEM for a slow decay of the coefficients with $\tilde{\sigma} = 2$ and a fast decay with $\tilde{\sigma} = 4$ are depicted in Figures 5–8. The amplitude $\bar{\alpha}$ in (8.2) was chosen as $\gamma/\zeta(\tilde{\sigma})$ with $\gamma = 0.9$, resulting in $\bar{\alpha} \approx 0.547$ for $\tilde{\sigma} = 2$ and $\bar{\alpha} \approx 0.832$ for $\tilde{\sigma} = 4$. Figure 5 shows the error estimator $\eta_{\mathcal{A}}$ and the reference error obtained by Monte Carlo sampling as described in Section 8.1 in the top row.

It can be observed that the rate of the error decay increases as expected for $p = 1$ to $p = 3$ large with P1 to P3. The respective rates are approximately the same as the decay rates of the error which is further verified in the graphs of the efficiency index $\eta_{\mathcal{A}}/\|e\|_{\mathcal{A}}$ in Figure 6. For $p = 1$ and $p = 2$, the efficiency lies in between 3 and 5 and becomes somewhat larger for $p = 3$. Asymptotically, for $p = 1, 2, 3$ an efficiency of 4 seems to be reached. The different behaviour of the adaptive algorithm in dependence of the polynomial FEM degree can be examined in the bottom row of Figure 5 which shows the number of active multi-indices and the number of mesh cells with respect to the total number of degrees of freedom. In case of $p = 1$, the spatial approximation error dominates and thus leads to a strong refinement of the mesh with relatively few stochastic modes being activated. On the opposite, the approximation error for $p = 3$ is small even for a coarse spatial discretisation, resulting in a dominating truncation error with respect to the stochastic modes. Consequently, the set of multi-indices grows strictly monotonically with each refinement step while the FEM mesh stays coarse. The relation of the energy error and the number of active stochastic modes is pictured in Figure 7. We also point out that while the $p = 1$ and $p = 3$ discretisations lead to (opposite) exclusive refinements, either of the physical or the stochastic space, the discretisation with $p = 2$ results in a dominating approximation error in the beginning which at a certain point reaches the same size as the stochastic truncation error. This can be observed by the addition of stochastic modes after 10^4 degrees of freedom (but not before).

Note that the graphs for the settings with slow and fast decay seem to be rather similar. However, there is a fundamental difference in the stochastic dimensions and the respective polynomial degrees activated for the anisotropic discrete stochastic space. We illustrate this in detail in Figure 8 where the active stochastic dimensions and the polynomial approximation order per

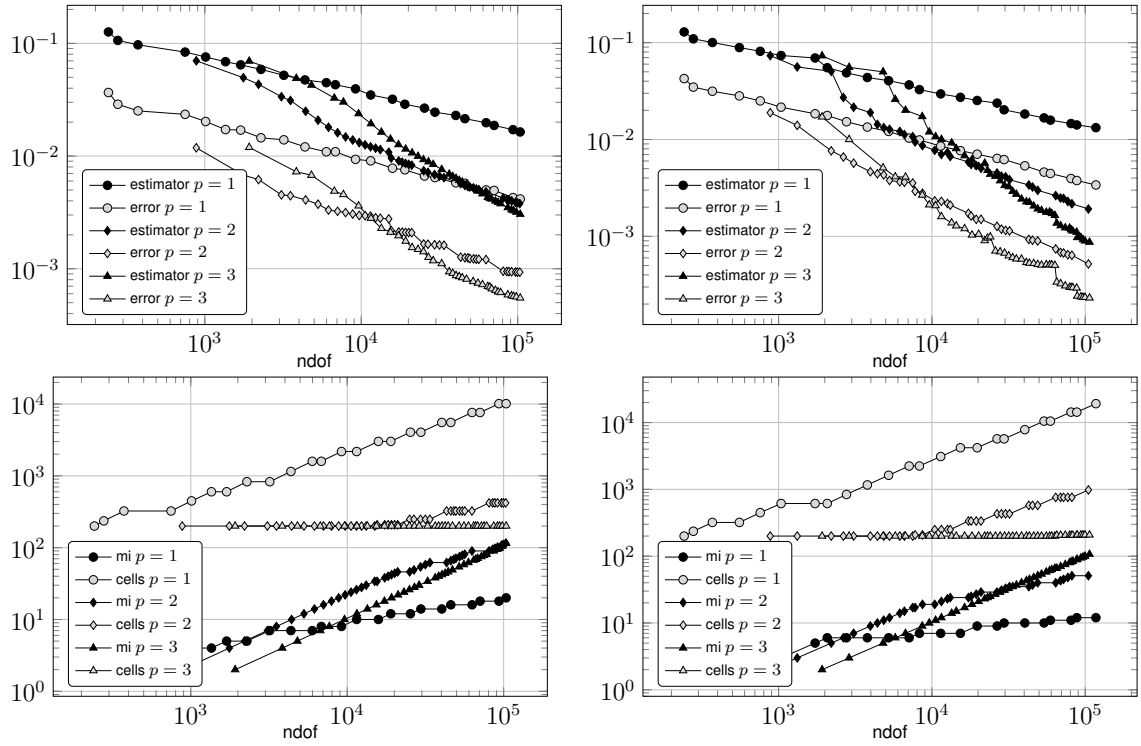

FIGURE 5. Convergence of the error estimator in the energy norm with FEM of degree $p = 1, 2, 3$ for the stationary diffusion problem on the square with homogeneous Dirichlet boundary conditions for slow ($\tilde{\sigma} = 2$, left) and fast ($\tilde{\sigma} = 4$, right) decay. Error estimator and sampled error (top) and cardinality of active set and number of mesh cells per active stochastic mode (bottom) for total number of degrees of freedom.

dimension is depicted. First, it can be observed that higher order FEM discretisations lead to the activation of more stochastic dimensions for the stochastic discretisation with both decay rates. Second, in case of slower decay, more stochastic dimensions are taken into account than with faster decay of the coefficient terms. With the $p = 3$ FEM, the slow decay setting yields 33 active stochastic dimensions with a maximum degree of 3 for the first stochastic dimension while this is degree 7 with the fast decay setting, leading to only 10 stochastic dimensions for approximately the same number of dofs. Since the first stochastic dimensions contain the most stochastic information of the coefficient, the polynomial degrees for their approximation is larger that for higher stochastic dimensions. In fact, for most active dimensions, a linear approximation seems to be adequate. This clearly shows that stochastic discretisations can greatly benefit from anisotropic problem adapted spaces.

8.2.2. *L-shaped domain.* A standard benchmark problem for deterministic a posteriori error estimators is the stationary diffusion problem (3.2) on the L-shaped domain $D = (-1, 1)^2 \setminus (0, 1) \times (-1, 0)$. It is well-known that the solution exhibits a singularity at the reentrant corner at $(0, 0)$ which has to be resolved by a pronounced mesh refinement in its vicinity in order to achieve optimal convergence rates. The previous remarks in Section 8.2.1 regarding the setup of the coefficient and the error evaluation are also valid with this example. The convergence of

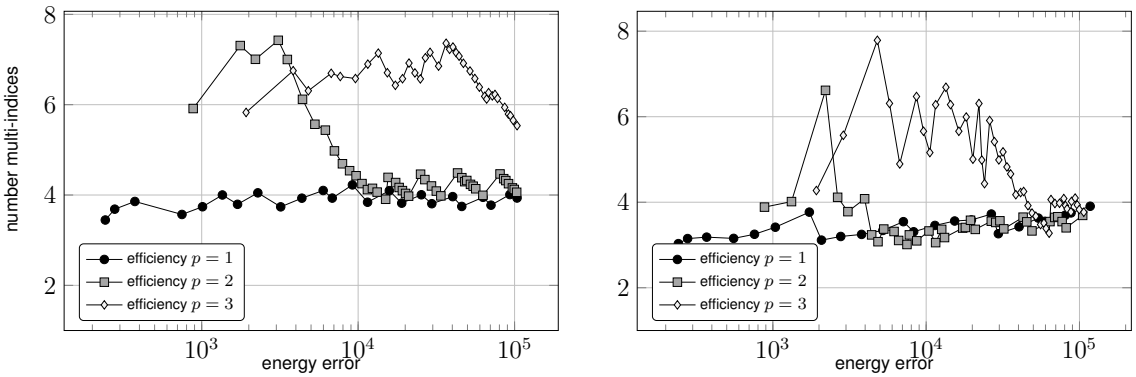

FIGURE 6. Efficiency indices of the error estimator in the energy norm with FEM of degree $p = 1, 2, 3$ for the stationary diffusion problem on the square with homogeneous Dirichlet boundary conditions for slow ($\tilde{\sigma} = 2$, left) and fast ($\tilde{\sigma} = 4$, right) decay.

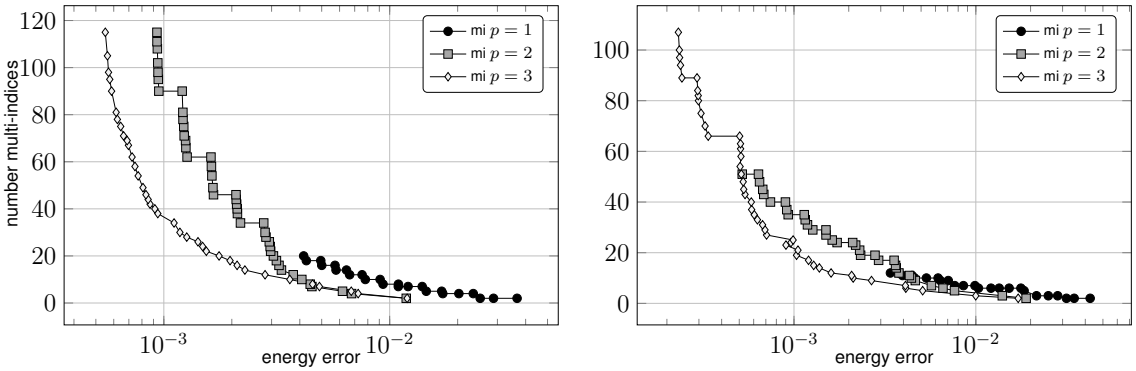

FIGURE 7. Number of active multi-indices with FEM of degree $p = 1, 2, 3$ for the stationary diffusion problem on the square domain with homogeneous Dirichlet boundary conditions for slow ($\tilde{\sigma} = 2$, left) and fast ($\tilde{\sigma} = 4$, right) decay with respect to the energy error.

the error estimator and its efficiency with regard to the error determined by (8.1) are depicted in Figures 9–12.

In comparison to the first stochastic example, the higher convergence rate for $p = 3$ FEM only becomes apparent after 10^4 dofs are reached, i.e., later than previously in the case of slow decay. Nevertheless, here and even more obvious in the setting with faster decay, the discretisation with $p = 3$ clearly exhibits the highest rate when compared with $p = 1, 2$. The error estimator in general performs better, i.e. more efficient, than in Section 8.2.1, as can be seen in Figure 10. Here, the efficiency indices lie at around 4 for all approximation orders and both coefficient parameters. Also note that, in contrast to the previous example, the mesh gets refined immediately for all polynomial degrees since the error caused by the singularity (i.e., the approximation error) dominates the overall error and first has to be reduced. Thus, the refinement of the mesh and the active set Λ is carried out quasi simultaneously for $p = 1, 2, 3$ as is depicted in Figure 9 (bottom row). The dependence of the energy error on the number of active stochastic modes is shown in Figure 11. Moreover, Figure 12 illustrates the maximum

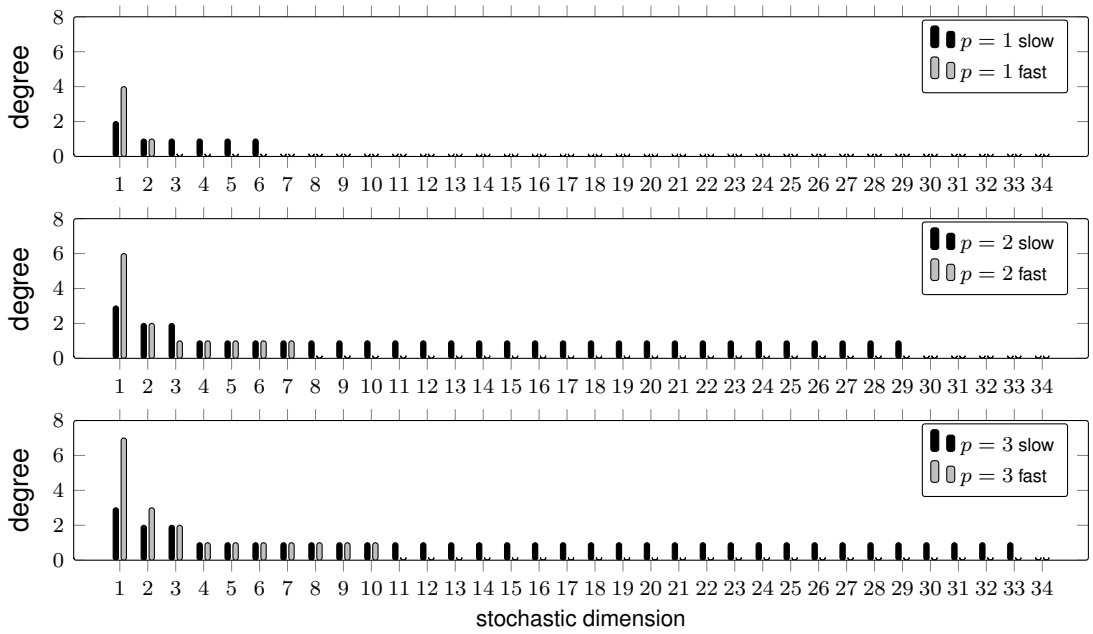

FIGURE 8. Polynomial degree for each stochastic mode with FEM of degree $p = 1, 2, 3$ (top to bottom) for the stationary diffusion problem on the square domain with homogeneous Dirichlet boundary conditions for slow ($\tilde{\sigma} = 2$) and fast ($\tilde{\sigma} = 4$) decay.

degrees of the activated stochastic dimensions after the last refinement step of the experiment. As before, the lowest order discretisation with $p = 1$ mainly has to improve the approximation quality of the physical space which results in a low number of stochastic dimensions being taken into account. For $p = 2, 3$ FEM, the stochastic spaces grow much larger. Again, for faster decay of the stochastic coefficients, the first stochastic dimensions carry the most information and hence require a more accurate approximation by the activation of larger degree polynomial chaos modes, namely up to degree 6 for $p = 3$. This leads to an anisotropic discretisation of the stochastic space since for most stochastic dimensions a lowest order discretisation apparently is sufficient.

Due to the adaptive refinement of the mesh, the otherwise degraded convergence rate (see experiments with uniform refinement in Section 2.4.1) is recovered by the resolution of the corner singularity. Again, the number of active stochastic modes increases substantially with the polynomial degree of the FEM while retaining rather coarse meshes.

REFERENCES

[1] M. AINSWORTH AND J. T. ODEN, *A posteriori error estimation in finite element analysis*, Pure and Applied Mathematics (New York), Wiley-Interscience [John Wiley & Sons], New York, 2000.

[2] I. BABUŠKA, F. NOBILE, AND R. TEMPONE, *A stochastic collocation method for elliptic partial differential equations with random input data*, SIAM J. Numer. Anal., 45 (2007), pp. 1005–1034.

[3] ———, *A stochastic collocation method for elliptic partial differential equations with random input data*, SIAM Rev., 52 (2010), pp. 317–355.

[4] I. BABUŠKA AND T. STROUBOULIS, *The finite element method and its reliability*, Numerical Mathematics and Scientific Computation, The Clarendon Press Oxford University Press, New York, 2001.

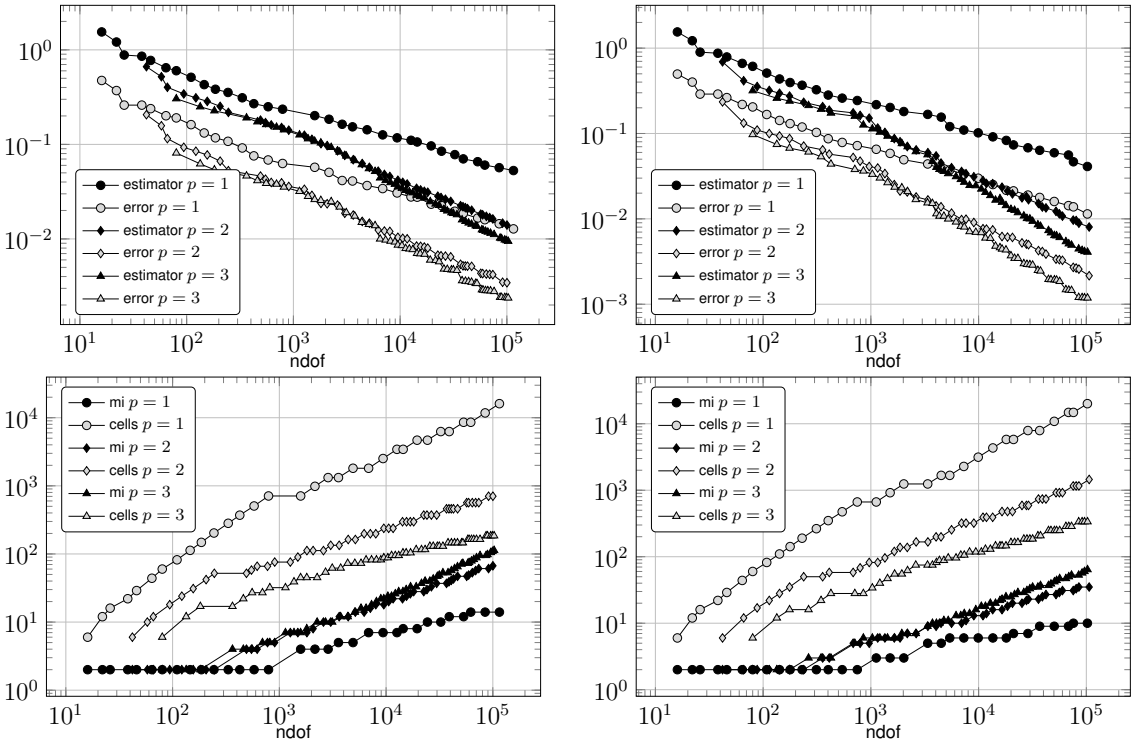

FIGURE 9. Convergence of the error estimator in the energy norm with FEM of degree $p = 1, 2, 3$ for the stationary diffusion problem on the L-shaped domain with homogeneous Dirichlet boundary conditions for slow ($\tilde{\sigma} = 2$, top) and fast ($\tilde{\sigma} = 4$, bottom) decay. Error estimator and sampled error (top) and cardinality of active set and number of mesh cells per active stochastic mode (bottom) for total number of degrees of freedom.

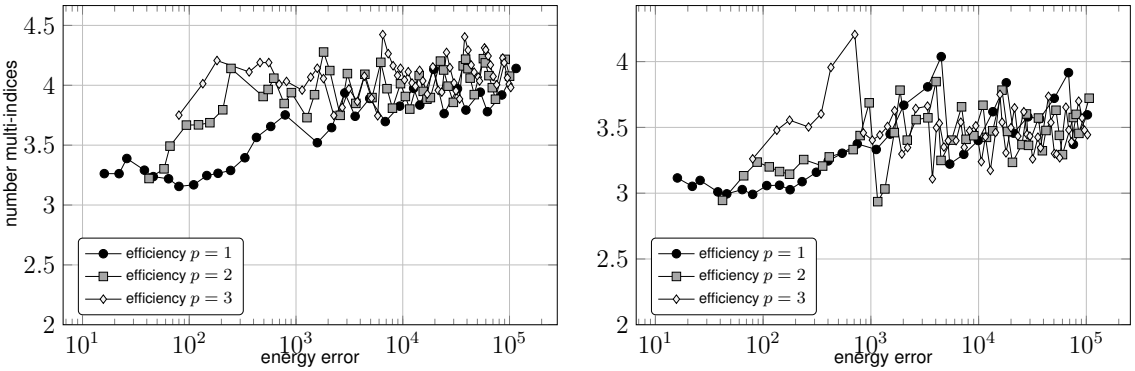

FIGURE 10. Efficiency indices of the error estimator in the energy norm with FEM of degree $p = 1, 2, 3$ for the stationary diffusion problem on the L-shaped domain with homogeneous Dirichlet boundary conditions for slow ($\tilde{\sigma} = 2$, left) and fast ($\tilde{\sigma} = 4$, right) decay.

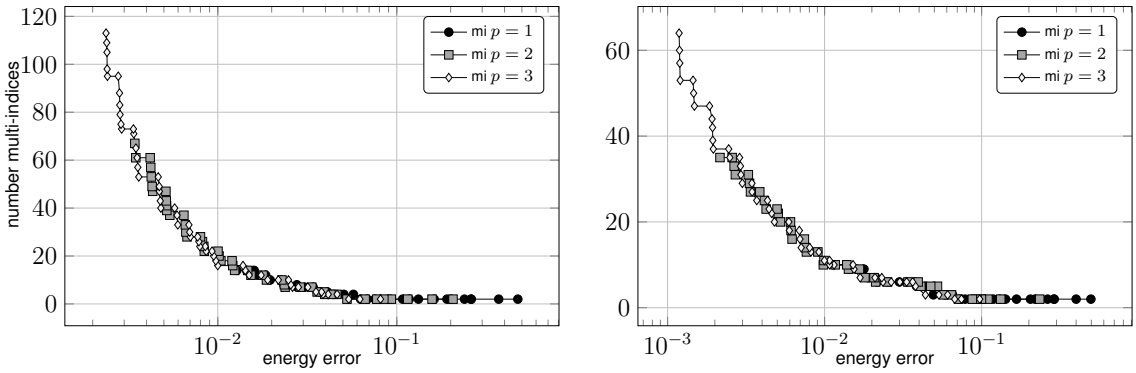

FIGURE 11. Number of active multi-indices with FEM of degree $p = 1, 2, 3$ for the stationary diffusion problem on the L-shaped domain with homogeneous Dirichlet boundary conditions for slow ($\tilde{\sigma} = 2$, left) and fast ($\tilde{\sigma} = 4$, right) decay with respect to the energy error.

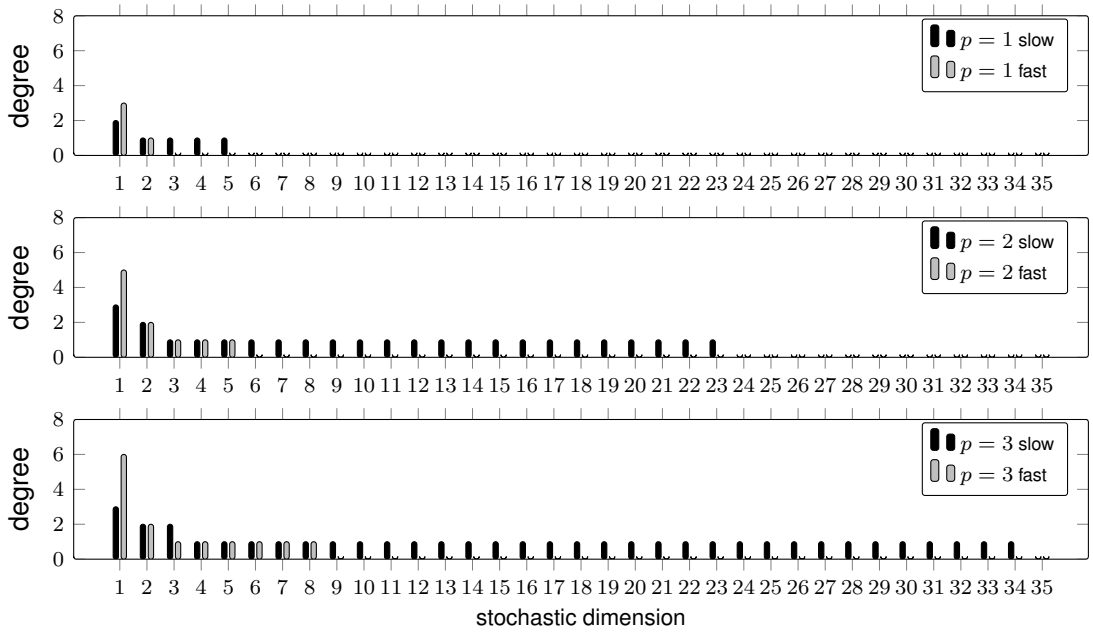

FIGURE 12. Polynomial degree for each stochastic mode with FEM of degree $p = 1, 2, 3$ (top to bottom) for the stationary diffusion problem on the L-shaped domain with homogeneous Dirichlet boundary conditions for slow ($\tilde{\sigma} = 2$) and fast ($\tilde{\sigma} = 4$) decay.

[5] S. BARTELS, C. CARSTENSEN, AND G. DOLZMANN, *Inhomogeneous Dirichlet conditions in a priori and a posteriori finite element error analysis*, Numer. Math., 99 (2004), pp. 1–24.

[6] A. BESPALOV, C. E. POWELL, AND D. SILVESTER, *Energy norm a posteriori error estimation for parametric operator equations*, SIAM J. Sci. Comput., 36 (2014), pp. A339–A363.

[7] M. BIERI AND C. SCHWAB, *Sparse high order FEM for elliptic sPDEs*, Comput. Methods Appl. Mech. Engrg., 198 (2009), pp. 1149–1170.

[8] D. BRAESS, *Finite elements*, Cambridge University Press, Cambridge, third ed., 2007. Theory, fast solvers, and applications in elasticity theory, Translated from the German by Larry L. Schumaker.

[9] D. BRAESS, V. PILLWEIN, AND J. SCHÖBERL, *Equilibrated residual error estimates are p-robust*, Comput. Methods Appl. Mech. Engrg., 198 (2009), pp. 1189–1197.

[10] D. BRAESS AND J. SCHÖBERL, *Equilibrated residual error estimator for edge elements*, Math. Comp., 77 (2008), pp. 651–672.

[11] F. BREZZI AND M. FORTIN, *Mixed and Hybrid Finite Element Methods*, Springer-Verlag New York, Inc., New York, NY, USA, 1991.

[12] C. CARSTENSEN AND C. MERDON, *Estimator competition for Poisson problems*, J. Comp. Math., 28 (2010), pp. 309–330 (electronic).

[13] ———, *Effective postprocessing for equilibration a posteriori error estimators*, Numer. Math, (2012).

[14] P. CHEN, A. QUARTERONI, AND G. ROZZA, *A weighted reduced basis method for elliptic partial differential equations with random input data*, SIAM J. Numer. Anal., 51 (2013), pp. 3163–3185.

[15] A. COHEN, R. DEVORE, AND C. SCHWAB, *Convergence rates of best N-term Galerkin approximations for a class of elliptic sPDEs*, Found. Comput. Math., 10 (2010), pp. 615–646.

[16] A. COHEN, R. DEVORE, AND C. SCHWAB, *Analytic regularity and polynomial approximation of parametric and stochastic elliptic PDE's*, Anal. Appl. (Singap.), 9 (2011), pp. 11–47.

[17] ———, *Analytic regularity and polynomial approximation of parametric and stochastic elliptic PDE's*, Anal. Appl. (Singap.), 9 (2011), pp. 11–47.

[18] P. DESTUYNDER AND B. MÉTIVET, *Explicit error bounds in a conforming finite element method*, Math. Comp., 68 (1999), pp. 1379–1396.

[19] M. EIGEL, C. J. GITTELSON, C. SCHWAB, AND E. ZANDER, *Adaptive stochastic Galerkin FEM*, Comput. Methods Appl. Mech. Engrg., 270 (2014), pp. 247–269.

[20] M. EIGEL, C. J. GITTELSON, C. SCHWAB, AND E. ZANDER, *A convergent adaptive stochastic Galerkin finite element methods*, Tech. Rep. 2014-01, Seminar for Applied Mathematics, ETH Zürich, 2014.

[21] M. EIGEL AND E. ZANDER, *ALEA - A Python Framework for Spectral Methods and Low-Rank Approximations in Uncertainty Quantification,* `https://bitbucket.org/aleadev/alea`.

[22] M. ESPIG, W. HACKBUSCH, A. LITVINENKO, H. G. MATTHIES, AND P. WÄHNERT, *Efficient low-rank approximation of the stochastic Galerkin matrix in tensor formats*, Comput. Math. Appl., 67 (2014), pp. 818–829.

[23] P. FRAUENFELDER, C. SCHWAB, AND R. A. TODOR, *Finite elements for elliptic problems with stochastic coefficients*, Comput. Methods Appl. Mech. Engrg., 194 (2005), pp. 205–228.

[24] R. G. GHANEM AND P. D. SPANOS, *Stochastic finite elements: a spectral approach*, Springer-Verlag, New York, 1991.

[25] C. J. GITTELSON, *Stochastic Galerkin approximation of operator equations with infinite dimensional noise*, Tech. Rep. 2011-10, Seminar for Applied Mathematics, ETH Zürich, 2011.

[26] W. HAN, *A posteriori error analysis via duality theory*, vol. 8 of Advances in Mechanics and Mathematics, Springer-Verlag, New York, 2005.

[27] R. S. LAUGESEN AND B. A. SIUDEJA, *Minimizing Neumann fundamental tones of triangles: an optimal Poincaré inequality*, J. Differential Equations, 249 (2010), pp. 118–135.

[28] H. G. MATTHIES, *Stochastic finite elements: computational approaches to stochastic partial differential equations*, ZAMM Z. Angew. Math. Mech., 88 (2008), pp. 849–873.

[29] H. G. MATTHIES AND A. KEESE, *Galerkin methods for linear and nonlinear elliptic stochastic partial differential equations*, Comput. Methods Appl. Mech. Engrg., 194 (2005), pp. 1295–1331.

[30] H. G. MATTHIES AND E. ZANDER, *Solving stochastic systems with low-rank tensor compression*, Linear Algebra Appl., 436 (2012), pp. 3819–3838.

[31] C. MERDON, *Aspects of guaranteed error control in computations for partial differential equations*, PhD thesis, Humboldt-Universität zu Berlin, 2013.

[32] F. NOBILE, R. TEMPONE, AND C. G. WEBSTER, *An anisotropic sparse grid stochastic collocation method for partial differential equations with random input data*, SIAM J. Numer. Anal., 46 (2008), pp. 2411–2442.

[33] ———, *A sparse grid stochastic collocation method for partial differential equations with random input data*, SIAM J. Numer. Anal., 46 (2008), pp. 2309–2345.

[34] A. NOUY, *Proper generalized decompositions and separated representations for the numerical solution of high dimensional stochastic problems*, Arch. Comput. Methods Eng., 17 (2010), pp. 403–434.

[35] S. REPIN, *A posteriori estimates for partial differential equations*, vol. 4 of Radon Series on Computational and Applied Mathematics, Walter de Gruyter GmbH & Co. KG, Berlin, 2008.

[36] C. SCHWAB AND C. J. GITTELSON, *Sparse tensor discretizations of high-dimensional parametric and stochastic PDEs*, Acta Numer., 20 (2011), pp. 291–467.

[37] R. A. TODOR AND C. SCHWAB, *Convergence rates for sparse chaos approximations of elliptic problems with stochastic coefficients*, IMA J. Numer. Anal., 27 (2007), pp. 232–261.

[38] R. VERFÜRTH, *A Review of a Posteriori Error Estimation and Adaptive Mesh-Refinement Techniques*, Teubner Verlag and J. Wiley, Stuttgart, 1996.